Study on Neural Mechanisms for Reaction Time Facilitation by Audio-Visual Integration

Junya Hirokawa

Department of Basic Biology, School of Life Science, The Graduate University for Advanced Studies

Division of Brain biology, National Institute for Basic Biology

March 2008

Contents

Chapter II:

Summary

Recent studies reveal that multisensory convergence can occur in early sensory cortical and subcortical areas. However, the behavioral importance of the multisensory integration in such areas is unknown. Here, I used c-Fos immunohistochemistry to explore neuronal populations specifically activated during the facilitation of reaction time induced by the temporally congruent audiovisual stimuli in rats. My newly developed analytical method for c-Fos mapping revealed a pronounced up-regulation of c-Fos expression particularly in layer 4 of the lateral secondary visual area (V2L) and the deep layer of superior colliculus (dSC). A local injection of a GABA A receptor agonist, muscimol, into dSC deteriorated the reaction time to all kinds of sensory stimuli but the audiovisual facilitation was not affected, suggesting that the dSC receives the integrated audiovisual information for the facilitated behavior. On the other hand, injection of muscimol into V2L completely suppressed the audiovisual facilitation of reaction time without affecting responses to unimodal stimuli. Such a selective suppression was not found following the injection of muscimol into the primary auditory and visual cortical areas. To examine whether or not the rats might have shown the facilitated responses because of increment of stimulus intensity caused by the two modal stimuli, the behavioral facilitation induced by the high-intensity unimodal stimuli was tested by the injection of muscimol into V2L, which turned out not to affect the facilitation. These results suggest that V2L, an early visual area, is integrating audiovisual information and is critically involved in the multisensory facilitation of reaction time.

Introduction

Animals have the ability to utilize information from different senses to gain behavioral advantages such as rapid responses (e.g. Hughes et al., 1994; Molholm et al., 2002; Corneil et al., 2002; Sakata et al., 2004) and increased accuracy (e.g. Stein et al., 1989; Frens and Van Opstal, 1995; Bolognini et al., 2005). Integration of different sensory information in the brain is considered to be a basic neural mechanism to produce the behavioral facilitation (Stein and Meredith, 1993). Conventionally, it had been considered that multisensory integration only occurs in higher-order association areas after extensive unimodal informational processing (e.g. Felleman and Van Essen, 1991). In agreement with this view, transient inactivation of higher-order cortical areas directly demonstrated their critical roles in the multisensory facilitation of spatial orientation accuracy in cats (Wilkinson et al., 1996; Jiang et al., 2002). However, if only higher cortical areas mediate enhanced responses to multisensory stimuli, such an extensive informational processing would inevitably take a long time. Thus, it may be speculated that there are different neural substrates for facilitating the speed of the behavioral response to multisensory stimuli.

The superior colliculus (SC) is well studied structure for multisensory integration because it contains many multisensory and sensorimotor neurons (e.g. Stein and Meredith, 1993; Zangenehpour and Chaudhuri, 2001; Bell et al., 2005; Holmes and Spence, 2005). Previous studies in anesthetized animals noted that the deep layers of the superior colliculus (dSC) showed enhanced or depressed activities to combination of auditory and visual stimuli compared with the sum of those to single auditory or visual stimulus (King and Palmer, 1985; Meredith and Stein, 1986; Meredith et al., 1987; Stein et al., 1988; Peck, 1996). Such firing properties of neurons correlated well with the behavior of animals (Stein et al., 1988; Stein et al., 1989), suggesting that the multisensory integration in the SC is fundamental to produce the behavioral facilitation (Stein and Meredith, 1993; Bell et al., 2005; but see Populin and Yin, 2002; Populin, 2005). Although previous studies revealed an important role of the

SC in the improvement of the accuracy of spatial orientation behaviors (Stein and Meredith, 1993), it is not studied whether the dSC also plays a critical role in facilitating the speed of behavioral response.

In addition to the dSC, a growing number of studies indicate multisensory processing in lower-order sensory cortical areas (see Ghazanfar and Schroeder, 2006 for review). Neuroimaging studies of primates revealed multisensory modulation in and near the primary sensory cortex (Calvert et al., 1997; Macaluso et al., 2000; Molholm et al., 2002; van Atteveldt et al., 2004; Kayser et al., 2005; Kayser et al., 2007), suggesting perceptual and attentional gains by such modulations. In addition, it was expected that the audiovisual interaction that correlates to the facilitation of reaction time occurs in the low-level sensory cortical area on the basis of the time course of the event-related brain potential in humans (Schroger and Widmann, 1998; Giard and Peronnet, 1999; Molholm et al., 2002; Murray et al., 2005; Sakowitz et al., 2005). However, the spatial resolution of neuroimaging analyses is not enough to determine the exact location of the source of activities at the cellular level. To compensate it, animal model is very useful if it is combined with brain mapping at higher spatial resolution and temporal inactivation of specific brain sites (e.g. Stein, 1998; Sakata et al., 2002). Under anesthetized conditions, electrophysiological studies directly confirmed multisensory integration in the presumptive unimodal sensory cortex (Schroeder and Foxe, 2002; Brosch et al., 2005; Lakatos et al., 2007), secondary sensory cortical areas (Di et al., 1994; Barth et al., 1995; Brett Green et al., 2003; Brett Green et al., 2004; Wallace et al., 2004). These findings are important in that they indicated the possible involvement of lower-order cortical areas in multisensory integration in awake animals. However, since anesthesia would have suppressed the normal intra-cortical processing, the involvement of these cortical areas for multisensory processing should be re-examined in awake animals.

To reveal the functional importance of multisensory integration in such lower-order sensory brain regions, a previous study in our laboratory developed a behavioral task for rats, in which the reaction times for auditory and visual stimuli can be accurately measured (Sakata et al., 2004). They found that the reaction time to audiovisual bimodal stimuli was shorter than that to either unimodal stimuli

(Sakata et al., 2004), suggesting that the behavioral system is useful to detect the behavioral facilitation by audiovisual integration in rats. In the present study, to identify the neural substrates of audiovisual behavioral facilitation, I conducted two types of experiment. First, I utilized the activity-dependent expression of c-Fos to map the neuronal population activated by the audiovisual facilitation of reaction time in the sensory cortex and subcortical regions (Chapter 1). Then, to determine the functional significance of neuronal activities in the brain regions identified by the c-Fos mapping, the effect of transient inactivation of the brain regions with muscimol on behavioral responses was examined (Chapter 2). I further confirmed that V2L is responding to the combination of cross modal stimuli but not to the degree of stimulus intensity of unimodal stimuli.

Chapter I:

Identification of neural substrates for multisensory facilitation by c-Fos mapping

Results

1) Facilitation of reaction time in a congruent audiovisual stimulus (cAV) task but not in temporally incongruent audiovisual stimulus (iAV) task

In this study, I used some two-alternative-choice tasks based on different audiovisual cue stimuli, slightly modifying the tasks reported in the previous paper (Fig. I-1A, Sakata et al., 2004). In these tasks, rats were trained to wait a stimulus presentation by holding their noses into a central hole (Fig. 1A). After the fore period, auditory and/or visual stimuli were presented from the left or right side. Rats discriminated the direction of the stimulus by poking their noses into a hole ipsilateral to the stimulus. The reaction time and accuracy of the discrimination were measured for each modality stimulus.

To identify neural substrates of the audiovisual facilitation of reaction time by c-Fos mapping, I designed two behavioral tasks (cAV and iAV tasks). In the cAV task, temporally congruent audiovisual stimuli were used as cue stimuli, whereas in the iAV task, the presentation was randomly delayed for 200 ms between auditory and visual stimuli. The delay period was chosen to be long enough to eliminate the audiovisual facilitation of reaction time (Fig. I-1B) but short enough not to cause double

reactions to both preceding and delayed stimuli. Two rat groups were trained extensively in either the cAV (n=10) or iAV (n=8) task (Fig. I-1C).

Both cAV and iAV task groups performed the final test session with more than 80% accuracy (cAV: 86% ±1.3; iAV: 84% ±1.3). In the cAV task group, the average reaction time in the final test session of the cAV task was significantly shorter than that in unimodal sessions during the course of the training period (Fig. I-1D). One-way repeated ANOVA indicated that the main effect of audiovisual congruency was significant ($F_{2,18}$=18.18, P<0.0001). In contrast, there were no significant differences in reaction times among the audiovisual and unimodal tasks in the iAV task group. These results suggest that only cAV task group achieved the facilitation of reaction time by audiovisual stimuli despite the fact that the amount of stimulus was same between the two groups. After the final session of the last tasks, each animal brain was immediately processed for c-Fos immunohistochemistry.

2) Standardization of rat neocortex and identification of cortical layers and areas

I compared c-Fos expression patterns between two groups that performed cAV and iAV tasks. However, it is difficult to accurately quantify c-Fos expression among different animals for a few reasons, especially in the cortex (see Discussion). To achieve objective and automatic procedures for the quantification of the spatial c-Fos expression pattern in a wide range of the cortex across different animals, here I developed an analytical method to standardize the images of cortical sections. The analysis was restricted to the posterior half of the cortex (Bregma distance from -4.3 to -8.0 mm), which has clear structural landmarks. The medial end of the white matter and the valley of the rhinal fissure were chosen as structural landmarks of the mediodorsal (MD) and the lateroventral (LV) ends of cortical sections, respectively (Fig. I-2A, B). The pial surface and the border between the cortex and the white matter were chosen as the outer contour (OC) and the inner contour (IC), respectively. The lengths of OC and IC were measured and equally divided into 100 points (Fig. I-2C). Sectors that were defined by every two adjacent points on each contour were extracted and converted to standardized rectangles by linear interpolation (Fig. I-2C). These rectangles from MD to LV were aligned from left

to right to form a standardized cortical section. These standardized cortical sections were aligned from the posterior to the anterior cortex to construct a "standardized cortical box" (Fig. I-2D). To analyze the spatial distribution of c-Fos expression at a particular layer, the specific layer fractions were extracted from the standardized cortical box (standardized layer map, Fig. I-2E).

To identify the cytoarchitectonic cortical layers, I analyzed layer profiles of gray level index (GLI) distribution on the standardized cortical sections processed by Nissl staining. GLI indicates the pixel intensity (gray values) of each image of Nissl staining, which reflects the density of neurons (Zilles et al., 1980; Schleicher and Zilles, 1990; Zilles et al., 1984). Because the relative positions of local peaks of GLI layer distribution was very similar across analyzed regions, especially at A1, V1 and V2L, I defined cytoarchitectonic layers in the standardized cortical sections as layer 1 (0-10% cortical depth), layer 2 (10-25% cortical depth), layer 3 (25-35% cortical depth), layer 4 (35-50% cortical depth), layer 5 (50-70% cortical depth) and layer 6 (70-100% cortical depth) (Fig. I-2F). Because the primary sensory areas have higher cell densities in layer 4 (Palomero-Gallagher and Zilles, 2004), the standardized layer-4 map (35-50% cortical depth) was constructed from the sections derived from both groups of rats (n=18) and the borders of cortical areas were delineated on this map by maximum local differences in mean GLI (white line in Fig. I-2G). The primary visual area (V1) and primary auditory areas (A1) were identified as the regions that had the highest cell densities, and these areas were separated by the low-GLI region, V2L. These delineated borders of cortical areas were highly consistent with those of the standard rat brain atlas (Paxinos and Watson, 1997).

3) c-Fos mapping in sensory cortex

I compared the density of c-Fos expression between the rats performed the cAV and iAV tasks by the standardizing method described above. The positive difference in normalized c-Fos-positive cell density between the two groups was evident at 35-50% of the mediodorsal-to-lateroventral distance and at Bregma distances of -6.80 to -6.04 mm, particularly in layer 4 and to a lesser extent in the infragranular layer (Fig. I-3A). Because only the cluster of c-Fos-positive signals in layer 4 satisfied

my statistical criteria (see Materials and Methods), I further analyzed the layer 4 signals. To determine the relationship of c-Fos distribution in layer 4 with cytoarchitectonic areas, I constructed the standardized layer-4 map from both c-Fos-immunostained and Nissl-stained sections for each task group. According to the cytoarchitectonic areal borders, the group-averaged c-Fos densities were particularly high in the primary visual and auditory sensory areas in both groups (cAV and iAV in Fig. I-3B). A prominent positive difference in the region between A1 and V1 was shown by subtracting the average c-Fos density in the iAV task from that in the cAV task in the standardized layer-4 map (Fig. I-3B). Up-regulation of c-Fos expression in layer 4 in the cAV task group was significant in a distinct area corresponding to the medial region of V2L ($P<0.05$, pixelwise unpaired *t*-test, Fig. I-3B). A representative photomicrograph of the V1/V2L border for each task shows increase of c-Fos expression especially in layer 4 of V2L and the V1/V2L border in the cAV task group compared with those in the iAV task group (Fig. I-3C). Consistent results were also obtained when the ROI was manually taken in only the medial region of V2L (Fig. I-3D). I confirmed that the consistency of cytoarchitectonic distributions between the cAV and the iAV task groups. The localization of the peak densities on the layer-4 map, particularly the V2L borders, closely matched those on the maps of the cAV and the iAV task groups (Fig. I-2G), suggesting no significant bias during standardization between the two groups.

4) c-Fos mapping in the superior colliculus (SC)

I also analyzed c-Fos expression in the SC, which involves the processing of auditory, visual and multisensory information (e.g. Stein and Meredith, 1993). I divided the SC into anterior and posterior parts for quantification because their sensory and motor representations are different (Redgrave et al., 1981; Dean et al., 1988a; Dean et al., 1988b). There were no significant differences in the superficial layer of the SC between the cAV and the iAV tasks (Fig. I-4A,B). On the other hand, the dSC in the cAV task group showed significantly higher c-Fos expression levels than that in the iAV task group in the anterior part (Fig. I-4A) but not in the posterior dSC (Fig. I-4B). Representative pictures of the

anterior SC for the cAV and the iAV tasks show that c-Fos in the cAV task is significantly up-regulated in the dSC (Fig. I-4C). These results suggest that the anterior dSC involves the facilitation of reaction time by audiovisual integration.

Discussion

1) Use of standardization method of cortical sections for functional mapping

c-Fos immunohistochemistry is a powerful tool for mapping the changes in neuronal activity caused by a behavioral outcome (Farivar et al., 2004 for review). It can provide information on entire-brain activation with high spatial resolution following a particular type of animal behavior. However, an objective, accurate and systematic comparison of c-Fos expression in the cortex between different individuals is very difficult because of individual differences in the brain morphology and staining quality. To circumvent these difficulties, several standardizing methods in the rodent brain have been proposed (e.g. Nguyen et al., 2004; Wada et al., 2006; Lein et al., 2006). Adding to these previously reported methods, here, I developed a new standardization method for analyzing the layer and areal distribution of c-Fos signals in the cortex. Since this method allowed me to directly compare layer profiles of c-Fos expression at particular cortical positions while visualizing the 3-D structure of the rat cortex at a glance. I was able to identify layer 4 of V2L as the specifically enhanced site of c-Fos expression during audiovisual behavioral facilitation.

Although this methodology is straightforward, there are two potential problems associated with standardization procedures to be discussed. First, since the standardized cortical sections are distorted toward deeper layers because the length of the outer contour is always longer than that of the inner contour (Fig. I-2C), the deviations among individual rats by these distortions decrease the statistical significance of the difference between the two groups in the deep layers compared with superficial layers. With this regard, it should be noted that the distortion was not so severe and the decrease in

statistical significance could be overcome using a larger dataset. Second, my method does not take into account individual variabilities in the size and location of functional areas, which may be caused by different behavioral experiences (Rutkowski and Weinberger, 2005). However, in my experiments the localizations of the averaged cytoarchitectonic areal borders on the standardized layer-4 map of two different groups were very similar (Fig. I-2G), suggesting that averaging cancelled out the individual variability of cytoarchitectonical areal distributions. In conclusion, my cortical standardization method is reliable enough to detect the differences in the expression levels of c-Fos and possibly other staining methods in the cortical areas at high resolution.

2) Neural substrates of multisensory behavioral facilitation

2-1) Lateral secondary visual area (V2L)

To identify the cortical region responsible for multisensory behavioral facilitation, I examined the regions that exhibit enhanced responses to congruent audiovisual stimuli (cAV task) compared with temporally incongruent stimuli (iAV task). In these tasks, experimental conditions such as total amounts of stimuli were set to be constant in two task groups, except for the difference of the stimulus presentation timing. Thus, the result of the subtraction should reflect a population of neurons specifically related to multisensory facilitation of reaction time induced by temporally congruent audiovisual stimuli.

I observed prominent up-regulations of c-Fos expression in the intermediate region between V1 and A1 (Fig. I-3B). Consistent with this result, electrophysiological mapping in anesthetized rats has revealed that the region between the visual and auditory sensory cortices is where superadditive interaction between auditory and visual stimuli occurs (Toldi et al., 1986; Barth et al., 1995; Wallace et al., 2004). In these studies, several distinct integration sites for auditory and visual stimuli are described. In my study, the distribution of c-Fos significantly deviated towards V1 (rightmost panel in Fig. I-3B), which is quite similar to the “POLYvis” area reported by Barth et al. (1995). The extrastriate cortex of rats has at least 7 distinct visual areas (Montero, 1993; Coogan and Burkhalter,

1993; Palomero-Gallagher and Zilles, 2004). Judging from the topographical locations as determined by the Nissl-GLI analysis, the region where the up-regulation of c-Fos expression was observed seems to overlap with the area lateromedial (LM) that occupies the second hierarchical level according to the laminar patterns of its connections with the striate and extrastriate visual areas (Coogan and Burkhalter, 1993). The medial region of V2L is activated by nonvisual stimuli in the rats that were enucleated early in life (Berninger et al., 2007) or rodents that have a reduced visual system (Bronchti et al., 2002; Piche et al., 2004; Campi et al., 2007). Therefore, the medial region of V2L might have multisensory processing capabilities and that might be involved in the multisensory behavioral facilitation.

Our laminar distribution analysis of c-Fos expression identified predominant activation in layer 4 of the medial region of V2L after the cAV task, suggesting the activation was caused by feedforward inputs of auditory and visual information from either primary sensory areas or thalamic nuclei (Coogan and Burkhalter, 1993). Feedforward inputs into layer 4 may be suited for coincidence detection because the activity of layer 4 has short duration (Wilent and Contreras, 2004). These results suggest that integration of auditory and visual information is conducted in the layer 4 of this region to produce facilitated reaction to bimodal stimuli. However, it should be noted that the c-Fos expression results do not exclude the possibility that the extra-granular layers or other cortical areas besides the medial region of V2L are involved in audiovisual integration. This is because c-Fos expression in neurons is effectively activated when EPSP and action potential are coincident (Mermelstein et al., 2000) and all neurons do not necessarily show the same degree of c-Fos activation (Sakata et al., 2002).

2-2) Activations of other cortical areas

In addition to the medial region of V2L, several distinct regions showing up-regulations of c-Fos expression were observed within V2L (Difference of cAV - iAV in Fig. I-3B), although those changes did not reach our statistical criteria (see Materials and Methods). One might argue that those distinct regions showing up-regulations of c-Fos expression might correspond to the other integration sites

reported in previous studies (Toldi et al., 1986; Barth et al., 1995; Wallace et al., 2004) or to the specific activities derived from known visual areas such as the areas laterointermediate (LI) and anterolateral (AL) (Espinoza and Thomas, 1983; Coogan and Burkhalter, 1993). It is interesting to reveal that the multisensory area corresponds to a specific retinotopic region within known unimodal areas or to a specific region where the multiple sensory modalities spatially overlap beyond the borders of those known areas.

2-3) Superior colliculus (SC)

I also observed a significant and specific c-Fos up-regulation in the dSC in the cAV task compared with that in the iAV task (Fig. I-4). This result is consistent with previous studies, which found that the dSC neurons response to a combination of different sensory stimuli greater than the sum of the responses to each unimodal stimulus (Meredith et al., 1987; Meredith and Stein, 1996). In our behavioral paradigm, the visual and auditory cues are presented in a peripheral space, which is represented in the posterior SC (Stein and Meredith, 1993). However, the major change of c-Fos in the cAV condition is not seen in the posterior dSC but seen in the anterior dSC (Fig. I-4). This result raises a possibility that the c-Fos up-regulation observed in the dSC was related to the maintenance of fixation rather than integration of sensory stimuli. Thus, the activation in anterior dSC may be driven by facilitation of reaction time followed by audiovisual integration in other part of brain. This hypothesis was tested by injecting muscimol into the anterior dSC in Chapter 2.

3) Consideration of the retinotopic maps in visual areas and SC

The differential map of c-Fos expression between the cAV and the iAV tasks also shows up-regulation of c-Fos expression in the layer 4 of the binocular area of V1 (Difference of cAV - iAV in Fig. I-3B), although only a small part of V1 achieved a statistical significance (*P*-value map in Fig. I-3B). This might indicate that coincident audiovisual stimuli presented from the peripheral visual field (azimuth 90°, elevation 0°) had evoked up-regulation of c-Fos expression in the nasal representation region of

the visual field in V1 and the corresponding region in V2L (the most medial region of V2L) (Espinoza and Thomas, 1983; Olavarria and Montero, 1984; Harvey and Worthington, 1990). This might be because c-Fos induction is highly effective when the dendritic EPSP and the action potential into the cell body are coincident (Mermelstein et al., 2000). Up-regulation of c-Fos in layer-4 neurons of V1 in the cAV task might be achieved by the coincident inputs of feedforward visual information into layer 4 and feedback information from V2L into extra-granular layers in V1 (Johnson and Burkhalter, 1996; Johnson and Burkhalter, 1997). Therefore, it is possible that feedback inputs modulate the visual activations of the nasal representation region in V1 (Coogan and Burkhalter, 1993; Johnson and Burkhalter, 1996; Johnson and Burkhalter, 1997; Angelucci and Bullier, 2003) and in turn, modulate the activity of the medial region of V2L that received feedforward inputs from V1. The medial region of V2L, which represents the nasal visual field, projects to the anterior part of the dSC (Olavarria and Van Sluyters, 1982; Olavarria and Montero, 1984; Harvey and Worthington, 1990), which involves the initiation of the nose-withdrawal response in rats (Sahibzada et al., 1986). Because the reaction time was measured when the animals withdrew their noses from the central hole in our system, the specific neural activation of the medial region of V2L might play an important role in facilitating the initiation of nose-withdrawal responses to audiovisual stimuli through the activation of the dSC (e.g., Meredith and Stein, 1985; King and Palmer, 1985; Bell et al., 2005). In consistent with this hypothesis, I observed up-regulation of c-Fos in the anterior dSC (Fig. I-4A). Further studies are necessary to determine the precise roles of the visual areas and dSC in the multisensory behavioral facilitation using a technique with high temporal resolution.

Figures

Figure I-1.

(A) Sequence of events for a trial. This figure is redrawn with slight modification from Fig. 1(A) in Sakata et al. (2004) with the permission of Springer Science and Business Media. The rats received target stimuli (visual and/or auditory) from the left or right side following nose poking into the central hole. They should poke their noses into the hole ipsilateral to the stimuli to receive a reward. (B) The rats (n=6) performed a task, in which the auditory and/or visual stimuli were redundantly presented at different times of onset (0, 50, 100, 150, 200, 300 ms). *P<0.05, statistically significant difference from the delay (0) (two-way analysis of variance (ANOVA), Tukey's post hoc analysis). (C) For c-Fos mapping, two task groups were used. In congruent audiovisual task (cAV), auditory and visual stimuli were simultaneously presented from the same place. In incongruent audiovisual task (iAV), auditory or visual stimuli were presented after visual or auditory stimuli, respectively with a delay of 200 ms. In the course of training period both groups of rats were trained by visual task (V) and auditory task (A). (D) The average reaction times in the audiovisual task (cAV or iAV task) of the final test sessions were compared with those in the unimodal tasks (auditory task (A) and visual task (V)) which were conducted during the course of the training period. *P<0.05.

Figure I-2.

(A) Representative photomicrograph of cortical section stained by antibody against c-Fos protein. (B) The local density of c-Fos-positive cells was computed and pseudocolored. The mediodorsal end (MD), lateroventral end (LV), inner contour (IC) and outer contour (OC) were manually chosen to extract part of the cortex. Scale bars, 1 mm (A, B) and 100 μm (insets in A, B). (C) The extracted cortex was divided into 100 bins (left; see Materials and Methods), and each bin was converted into a standard rectangle (left to center as shown by thick arrows). The standardized rectangular bins were orderly reassembled into a stripe to form a standardized cortical section (right). (D) Standardized

cortical sections were assembled from the posterior section to the anterior section to form a standardized cortical box. (E) A specific layer fraction (layer 4, for example) from a standardized cortical box was extracted to construct a standardized layer map. (F) The graph shows the average gray level index (GLIs) layer profiles of the Nissl-stained sections (Bregma -5.6) at the lateral secondary visual area (V2L), primary visual area (V1), primary auditory area (A1) and pooled data (all). (G) Standardized layer-4 maps (35-50% in cortical depth) of average Nissl GLI were constructed for the both task groups (all), the congruent audiovisual (cAV) task and temporally incongruent audiovisual (iAV) task groups. Note that areal delineation (white lines and abbreviations) closely matches between the two groups.

Figure I-3.

(A) Each horizontal stripe shows the standardized cortical section of group averaged c-Fos density at the Bregma distance indicated on the left for the congruent audiovisual (cAV) and temporally incongruent audiovisual (iAV) tasks. The right two figures show the differential map (cAV-iAV) and *P*-value map between the cAV and iAV task groups ($P<0.05$, *t*-test). (B) The standardized layer-4 maps of average c-Fos density for each task group (cAV and iAV) and the differential map between them (cAV-iAV) and *P*-value map ($P<0.05$, *t*-test). White lines indicate the boundary of cortical areas, which were identified on the basis of the cytoarchitectonic distribution (Fig. I-2G). (C) Representative photomicrographs of c-Fos staining within the visual cortex of rats from the cAV and iAV task groups. Scale bars, 250 μm. (D) The layer distribution of the average c-Fos-positive cell density in the medial region of V2L (Bregma 4.8 to 6.8 mm) in the cAV and iAV tasks were quantified by conventional region of interest (ROI) analysis. Unpaired *t*-tests were performed for the comparison between the task groups, $*P<0.05$.

Figure I-4.

(A-B) The left coronal diagrams (adapted from Paxinos and Watson, 2004) show the region of

interests (ROIs) for counting c-Fos-positive cells at the anterior (A) and posterior (B) part of superior colliculus (SC). ROIs were selected from the superficial (s1-s3) and deep (d1-d4) layers of SC. The shaded region indicates deep layers of SC (dSC). The right figures show average densities of c-Fos-positive cells in each ROI of SC (s1-s3, d1-d4) after the cAV and iAV tasks at the anterior (A) and posterior (B) part of SC. Unpaired *t*-tests were performed for the comparison between the task groups, $*P<0.05$. (C) Representative photomicrographs of c-Fos expression after the cAV (left) and iAV (right) tasks at the anterior part of SC. Dashed lines indicate the borders of the deep layers. Scale bars, 1 mm

Fig. I-1

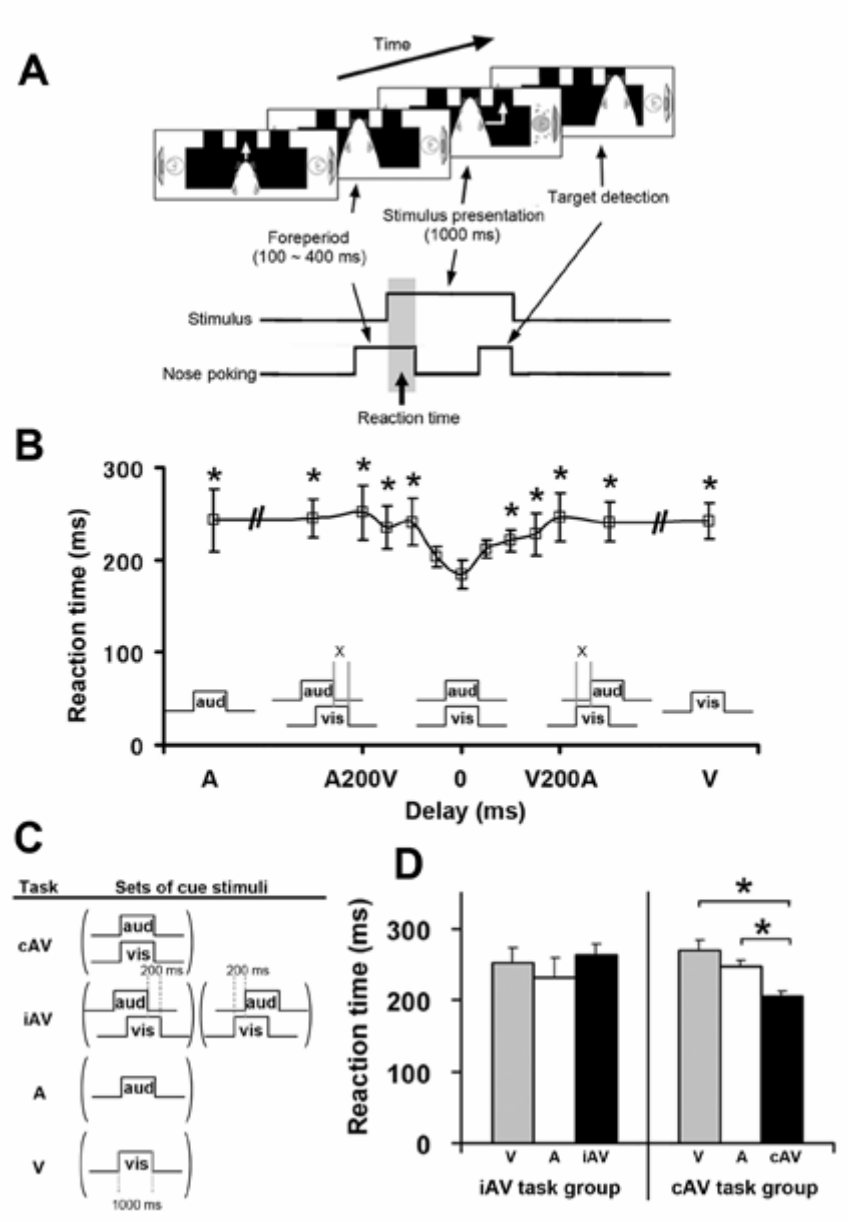
A
Time
Target detection
Stimulus presentation
(1000 ms)
Foreperiod
(100 ~ 400 ms)
Stimulus
Nose poking
Reaction time
B
Reaction time (ms)
300
200
100
0
aud
vis
X
A
A200V
0
V200A
V
Delay (ms)
C
Task
Sets of cue stimuli
cAV
iAV
A
V
200 ms
1000 ms
D
Reaction time (ms)
300
200
100
0
V
A
iAV
cAV
iAV task group
cAV task group

Fig. I-2

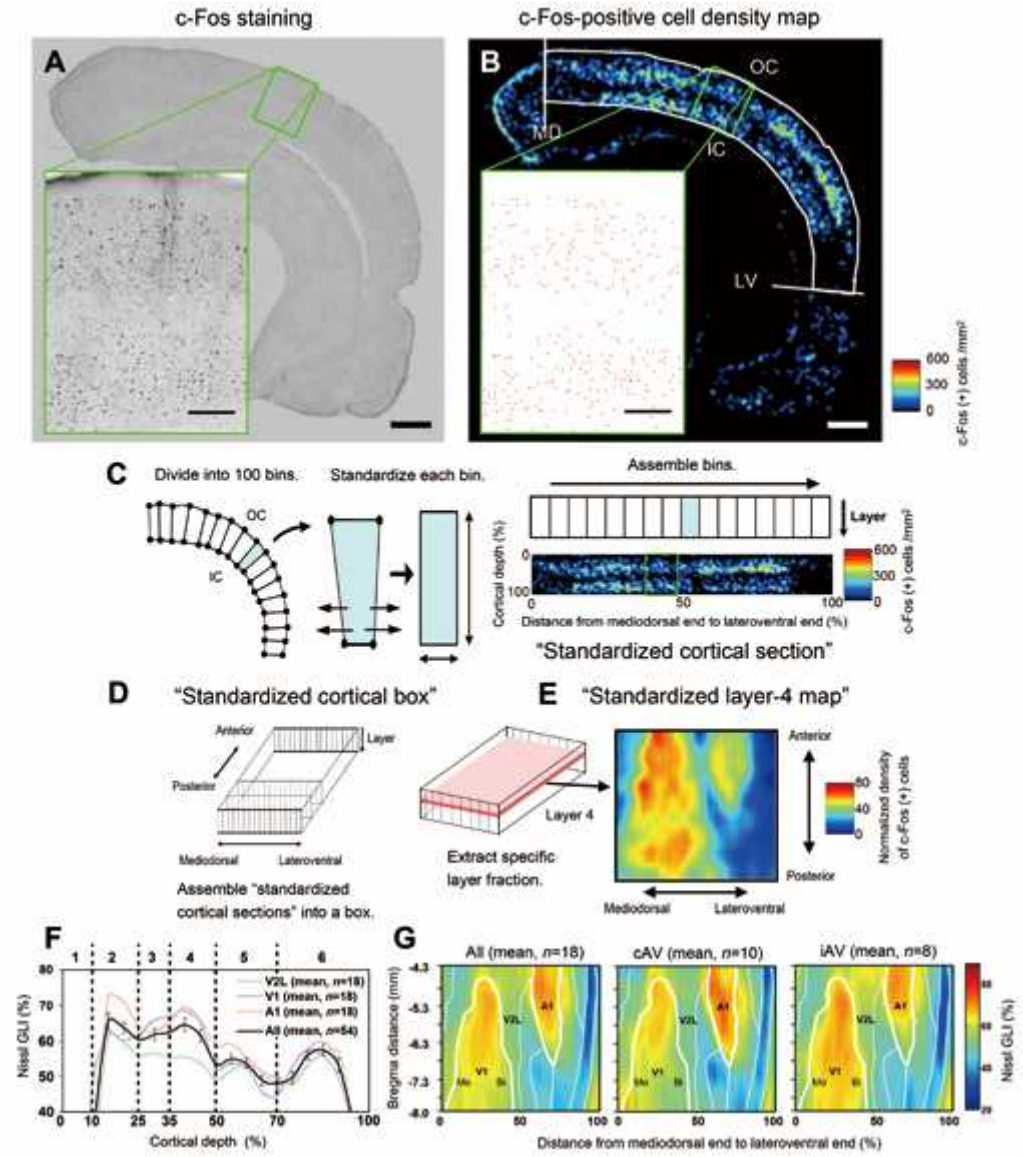
c-Fos staining
c-Fos-positive cell density map
A
B
OC
MD
IC
LV
600
300
0
c-Fos (+) cells /mm²
C
Divide into 100 bins.
Standardize each bin.
Assemble bins.
OC
IC
Layer
Cortical depth (%)
0
100
0
50
100
Distance from mediodorsal end to lateroventral end (%)
"Standardized cortical section"
D
"Standardized cortical box"
Anterior
Posterior
Layer
Mediodorsal
Lateroventral
Assemble "standardized cortical sections" into a box.
E
"Standardized layer-4 map"
Layer 4
Extract specific layer fraction.
Anterior
Posterior
Mediodorsal
Lateroventral
Normalized density of c-Fos (+) cells
F
1
2
3
4
5
6
V2L (mean, n=18)
V1 (mean, n=18)
A1 (mean, n=18)
All (mean, n=54)
Nissl GLI (%)
Cortical depth (%)
G
All (mean, n=18)
cAV (mean, n=10)
iAV (mean, n=8)
Bregma distance (mm)
Distance from mediodorsal end to lateroventral end (%)
Nissl GLI (%)

Fig. I-3

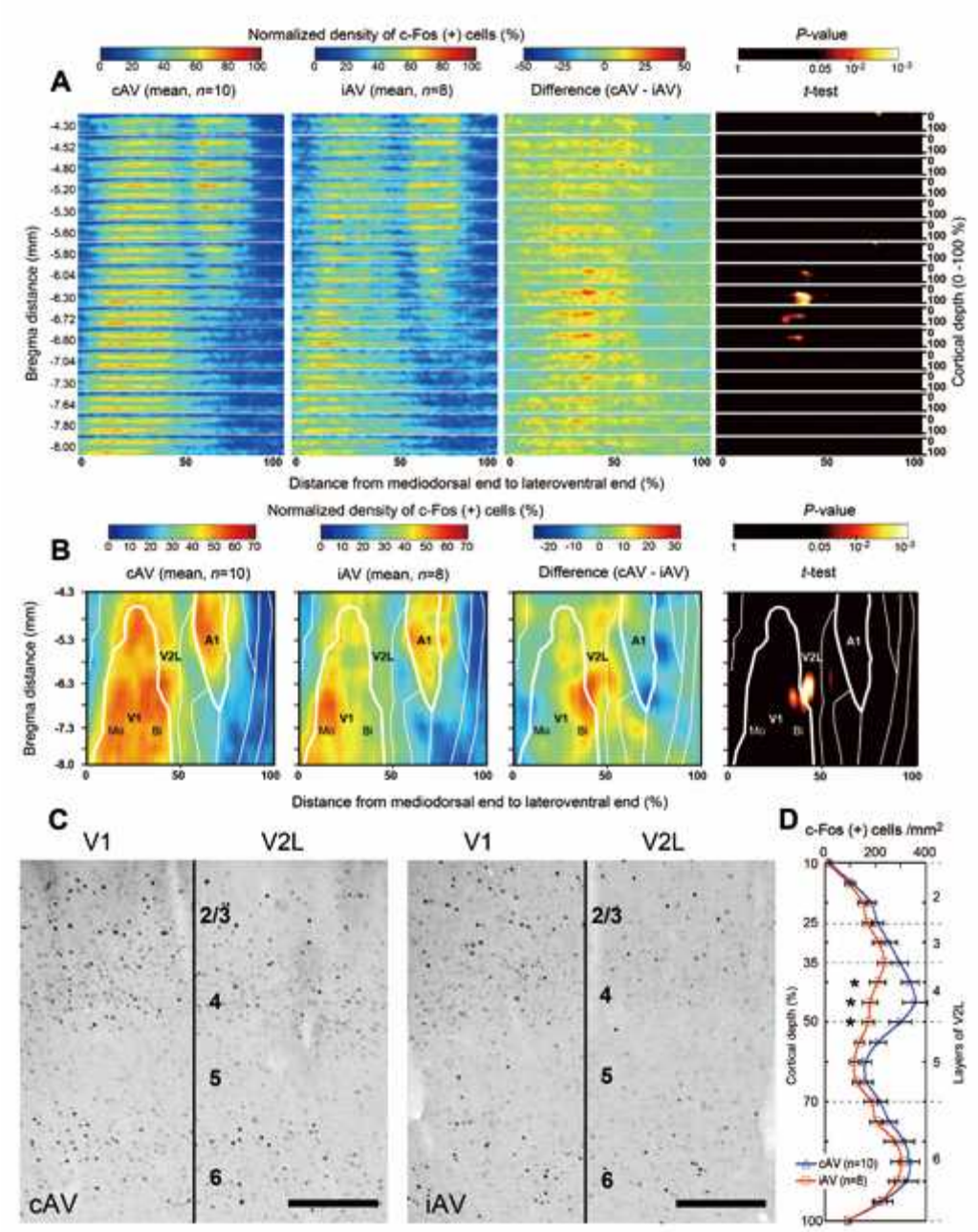
A
Normalized density of c-Fos (+) cells (%)
cAV (mean, n=10)
iAV (mean, n=8)
Difference (cAV - iAV)
P-value
t-test
Bregma distance (mm)
Cortical depth (0 -100 %)
Distance from mediodorsal end to lateroventral end (%)
B
Normalized density of c-Fos (+) cells (%)
cAV (mean, n=10)
iAV (mean, n=8)
Difference (cAV - iAV)
P-value
t-test
Bregma distance (mm)
V1
V2L
A1
Mo
Bl
Distance from mediodorsal end to lateroventral end (%)
C
V1
V2L
V1
V2L
2/3
4
5
6
cAV
iAV
D
c-Fos (+) cells /mm2
Cortical depth (%)
Layers of V2L
cAV (n=10)
iAV (n=8)

Fig. I-4

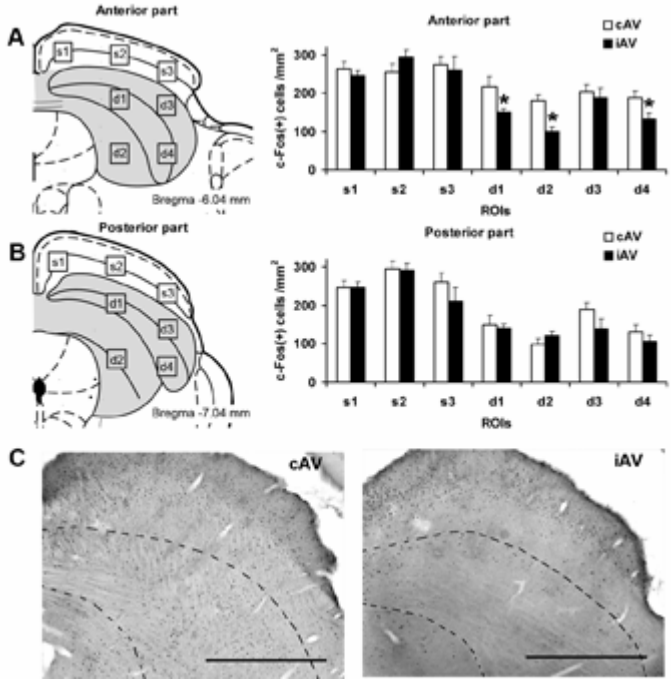
A
Anterior part
s1
s2
s3
d1
d3
d2
d4
Bregma -6.04 mm
Anterior part
cAV
iAV
c-Fos(+) cells /mm²
300
200
100
0
s1
s2
s3
d1
d2
d3
d4
ROIs
B
Posterior part
Bregma -7.04 mm
Posterior part
C
cAV
iAV

Chapter II:

Roles of early cortical areas and superior colliculus in multisensory behavior

Results

1) Effect of dSC inactivation on the reaction time facilitation

To evaluate the contribution of SC to the audiovisual facilitation of reaction time, I injected muscimol into the anterior dSC, where c-Fos expression level specifically increased in the cAV task (Fig. I-4). Since the results in the bilateral inactivation were not consistent and the consequent behavior of the rats was chaotic, probably depending on the balance of muscimol diffusion between the two sides of SC (Kilpatrick et al., 1982), I injected muscimol into one side and saline into the other side to test the performance in the A-V-cAV task (Fig. II-1A).

Unilateral muscimol injection into dSC caused two types of behavioral deficiency for each modality stimulus: decrease of the success rate and increase of the reaction time. In this task, three types of errors were possible: "false alarm", withdrawal from the central hole before the onset of the target stimulus; "false hit", a nose poke into a hole other than the correct hole; and "miss", failure to respond to either hole within 2,500 ms from the onset of the target stimulus. The "false alarm" error did not differ in any conditions and any brain regions between those of the rats injected muscimol and saline (data not shown). The analysis of the error types revealed that the number of "false hits" generally increased in the hemifield contralateral to the muscimol-injection sides in comparison with those in the

hemifield ipsilateral to the injection sides (Fig. II-1B). In addition, the numbers of "miss" errors in response to the visual and audiovisual stimuli presented to the contralateral hemifield also increased (Fig. II-1B). In parallel with the increases of "miss" error rates, movement time, which was defined as the time between withdrawing the nose from the central hole and poking it into the correct hole, also significantly increased for audiovisual and visual stimuli but not for auditory stimuli (Fig. II-1C). These contralateral "neglects" of sensory stimuli were consistent with previous reports (Kilpatrick et al., 1982; Dean and Redgrave, 1984; Burnett et al., 2004; Stein and Meredith, 1993). Increases in the number of "misses" were particularly evident for responses to the audiovisual stimuli (AV: 6.26% ±1.38) rather than for those to unimodal stimuli (V: 2.73% ±0.75, A: 1.50% ±0.72). The main effect of one-way repeated-measures ANOVA was statistically significant ($F_{2,16}$=9.71, P=0.0017; with post hoc Tukey HSD test, AV VS V: P =0.016, AV VS A: P=0.0018, V VS A: P=0.53). The specific defect on orientation response to audiovisual stimuli suggests that the orientation movement for audiovisual stimuli is critically dependent on the function of SC.

In addition to the increases of errors, the average reaction time for stimuli presented to the contralateral hemifield generally increased following the muscimol injection in all three combinations of modalities (Fig. II-1D), suggesting that SC is involved in the initiation of orientation, irrespective of stimulus modality. To evaluate the extent of reaction time facilitation by bimodal stimuli, the cumulative probability distribution of reaction time was analyzed (Fig. II-1E). Surprisingly, the rats still reacted faster to contralateral audiovisual stimuli than to unimodal stimuli even under this contralateral-neglect condition after the muscimol injection (Fig. II-1E). To quantify the effect of muscimol on audiovisual facilitation, audiovisual facilitation index (F_{AV}), defined as the difference between bimodal and shorter unimodal reaction times (indicated by yellow areas in Fig. II-1E), was calculated for each rat (see Materials and Methods). The indices of the audiovisual facilitation slightly increased instead of decreasing (ipsilateral side, 5.18% ±0.82; contralateral side; 9.69% ±2.72, respectively; Wilcoxon signed rank test; P=0.05) after the muscimol injection (Fig. II-1E). These results suggest that SC is involved in the initiation of a reaction to any sensory stimuli but is not

essential for the audiovisual facilitation of the reaction time of nose withdrawal.

I examined c-Fos expression after the task performance in subsets of rats treated with muscimol and saline (3 to 4 rats for muscimol and 2 to 3 rats for saline in each injection group), because the use of c-Fos immunohistochemistry to estimate the suppressive effects of muscimol is established (Wang and Redgrave, 1997). The spread of muscimol around the injection sites was estimated by visually assessing the region exhibiting the loss of normal c-Fos staining in the sections. The placements of cannula tips in SC were verified to be within 1 mm of the targeted place of dSC. The inactivated area was primarily restricted to the anterior of the medial SC as verified by c-Fos expression (Fig. II-2A). The comparison of c-Fos expression level between the muscimol- and saline-injected hemispheres revealed that c-Fos expression level decreased statistically significantly in the anterior of the medial dSC as well as in the superficial layer of SC (Fig. II-2B,C). On the other hand, there was no significant decrease in the posterior dSC (Fig. II-2D).

2) Effect of V2L inactivation on the reaction time facilitation

Next, I examined the effect of bilateral injection of muscimol into V2L by the performance of the A-V-cAV task (Fig. II-3A). Because the behavioral consequence of V2L inactivation was unknown, I also injected muscimol into primary auditory (A1) and visual (V1) areas as controls for determining the proper amount of muscimol into cortex (Talwar et al., 2001; Gerstein et al., 2002; Smith et al., 2004). The inactivation of these cortical areas deteriorated the success rate and the reaction time in modality specific manners. The increased type of errors after muscimol injections into these cortical areas was only the modality-specific "false hit". "Miss" errors were not affected by the injection of muscimol in any cortical areas.

The injection of muscimol into V1 specifically delayed the reaction time for visual stimuli (P=0.0083, Fig. II-3C) and the negative effect on the success rate for visual stimuli was very close to the significant level (P=0.054, paired t-test, Fig. II-3B). On the other hand, the same amount of muscimol injected into A1 produced an auditory-specific effect on the success rate in the A-V-cAV task (Fig.

II-3B), but the reaction time for auditory stimuli was not significantly affected (P=0.211, paired t-test, Fig. II-3C).

The injection of the same amount of muscimol into V2L did not significantly affect the success rate for any modality stimuli (Fig. II-3B). In contrast, the reaction time for audiovisual stimuli was specifically increased by muscimol injection into V2L, whereas that for auditory or visual stimuli was not affected (Fig. II-3C). In the case of the saline injection, the cumulative probability of the reaction time in the audiovisual trials was shifted toward shorter-time points than that in the unimodal auditory or visual trials (Fig. II-3D, upper), as previously shown (Sakata et al., 2004), confirming the audiovisual facilitation of the reaction time in the A-V-cAV task. Bilateral muscimol injection into V2L caused a shift of the cumulative probability of the reaction time for audiovisual stimuli to similar probability distribution of faster unimodal responses (Fig. II-3D, lower). In the case of saline injection into V2L, the average F_{AV} was 7.7%, which decreased to 0.4% following the muscimol injection into V2L (Fig. II-3D, P=0.018, Wilcoxon signed rank test). Bilateral muscimol injection into V1 also significantly decreased F_{AV} (7.2 to 2.8%, P=0.028, Wilcoxon signed rank test). In contrast, the decrease of F_{AV} after A1 inactivation was not large and did not reach significance (8.8 to 6.8% P=0.074, Wilcoxon signed rank test).

Injection of muscimol produced loss of c-Fos expression around cannula tips (Fig. II-4A). The center of the inactivation common to all rats was located within the target regions (Fig. II-4B for summary diagrams and Fig. II-4C for c-Fos quantification). The ranges of inactivation for V2L and A1 were located between bregma -4.8 and -6.8 mm. The range of inactivation for V1 was mainly restricted within the medial region of V1 (monocular area of V1; V1M) between bregma -6.3 and -8.3 mm and did not invade into V2L (Fig. II-4B). On the other hand, A1 inactivation often showed partially suppressed c-Fos expression at the lateral part of V2L but the medial part of V2L was not affected.

3) Effect of inactivation of V2L on intensity-related unimodal facilitation

Behavioral performance depends on stimulus intensity (Murray et al., 2001; Bushnell et al., 2003;

Patching and Quinlan, 2004). Indeed, the reaction time to unimodal stimuli was delayed when the intensities of the stimuli were lowered (Fig.II-5B). I named this type of response facilitation induced by the increased intensities of unimodal stimuli as F_{UNI} (intensity-related unimodal facilitation), which is in contrast to audiovisual facilitation (F_{AV}) (see Materials and Methods). In the A/V/cAV task, the amount of stimuli in the cAV trial, which received auditory plus visual stimuli, can be larger than those in the A and the V trials, which received only auditory and visual stimuli, respectively. Thus this raised a question as to whether the facilitation of reaction time is due to the convergence of cross modal stimuli or due to the increased intensity of two modal stimuli. I therefore examined the effect of muscimol injection into V2L on the intensity-related unimodal facilitation. In a session in which normal- or low-intensity sensory stimuli were randomly presented (Fig. II-5A), both audiovisual and intensity-related unimodal facilitations were observed (Fig. II-5B and C, left panel). The muscimol injection into V2L suppressed audiovisual facilitation (Fig. II-5C right panel) in comparison with the saline injection. On the other hand, the intensity-related unimodal facilitation was not affected by the muscimol injection into V2L (Fig. II-5B right panel). These results suggest that audiovisual and intensity-related unimodal facilitations are controlled by different neural mechanisms and that V2L specifically mediates the audiovisual facilitation. Histological analysis confirmed the suppressed region of c-Fos expression by muscimol was restricted in the vicinity of V2L (Fig. II-6A) and the c-Fos expression level at V2L in the muscimol-injected animals was significantly lower than that in the saline-injected animals (Fig. II-6B).

Discussion

1) Functional role of lateral secondary visual area (V2L)

Bilateral injections of muscimol into primary sensory cortical areas reduced the success rate and delayed the reaction time in a modality specific manner. Because errors made by rats after inactivation of primary sensory areas were mostly false-hit errors, rats randomly poked their noses regardless of the side of holes rather than idled when they could not discriminate the direction of the stimuli. Therefore, inactivation of primary cortical areas did not deteriorate their motor function or motivation. These sensory-specific effects confirmed that the amount of muscimol used was appropriate for examining the selective function of cortical areas.

The same amount of muscimol into the region including the medial region of V2L specifically suppressed the audiovisual facilitation of the reaction time without affecting the reaction time to unimodal stimuli, suggesting a specific role of V2L in multisensory behavioral facilitation. Lesion studies of the region including the medial part of V2L demonstrated the role of the area in visual complex pattern discrimination but not simple ones (McDaniel et al., 1982; Pinto Hamuy et al., 2004). Because pattern discrimination ability was not required for rats in my task, it is not surprising that rats can still respond to visual stimuli after inactivation of V2L in my experiments. The extent of muscimol spread which was determined on the basis of c-Fos expression was affected not only in the medial region of V2L but also in the lateral region: the potential association areas adjacent to A1 (including parietal association cortex (PtA), secondary auditory area, dorsal cortex (AuD) and temporal association cortex (TeA) in Paxinos and Watoson (1997)) (Fig. II-4B). Therefore, although it is possible that the suppression of bimodal-stimulus-specific responses is attributed to the dysfunction of these association areas, the injection of muscimol targeting A1, which significantly affected c-Fos expression in those areas (Fig. II-4B), did not affect the reaction time to bimodal stimuli (Fig. II-3C).

Taken together with the c-Fos mapping data, the medial region of V2L is a critical site for producing facilitated reaction time responding to bimodal stimuli.

2) Behavioral facilitation mediated by lateral secondary visual area (V2L)

It has been argued that the bimodal facilitation that shortens the reaction time for either modality stimuli does not necessarily require bimodal integration in the brain. For example, the facilitation of reaction time to audiovisual stimuli may be simply due to the increased probability of neuronal responses owing to redundant cues (i.e. auditory plus visual stimuli). This type of statistical facilitation can be expressed by the race model (e.g. Miller, 1982; Wenger and Townsend, 2000; Molholm et al., 2002; Patching and Quinlan, 2004), in which two modal sensory signals race along separate pathways toward a common site that generates a response, and the winning modality triggers the response. Using this model, the probabilities of facilitated responses to bimodal stimuli are predicted by a linear summation of unimodal response probabilities. Although the averaged cumulative probability of reaction time to bimodal stimuli was within the prediction of the model (data not shown), this does not necessarily mean that neural interactions between auditory and visual information did not occur. Indeed, we found that V2L inactivation specifically inhibited bimodal responses without affecting unimodal responses. This phenomenon cannot be explained by the race model, because it assumes that a bimodal response is produced by one of two unimodal stimuli. One could also argue that the facilitation was caused by a higher intensity of stimuli regardless of their cross-modality. This was not the case either, because the inactivation of the V2L region specifically suppressed enhanced responses induced by the combination of different modality stimuli but not by that of unimodal stimuli with a high degree of intensity. Taken together, our experiments suggest that the facilitation of reaction time is produced by multisensory interaction of auditory and visual stimuli in the brain and V2L plays a critical role in this process.

3) Anatomical substrates of multisensory facilitation of reaction time

As consistent with previous studies (e.g. Corneil et al., 2002; Hairston et al., 2006; Whitchurch and Takahashi, 2006), I confirmed that the spatial localization accuracy (measured as success rate) and response speed (measured as reaction time) did not correlate in the performance of A-V-cAV task, suggesting that these two performances are controlled by different neural mechanisms. Indeed, inactivation of A1 did not significantly deteriorate the reaction time to auditory stimuli (Fig. II-3C), despite the fact that the lateralization ability to auditory stimuli was largely defected (Fig. II-3B), as consistent with previous reports (Talwar et al., 2001; Smith et al., 2004). Thus, spatial localization accuracy to auditory stimuli is controlled by the information through A1 but the rapid response to auditory stimuli depends on subcortical regions (e.g. Goodale and Murison, 1975; Leitner and Cohen, 1985; Koch and Schnitzler, 1997; Komura et al., 2005) rather than the cortex. Consistently, A1 inactivation did not suppress the reaction time to audiovisual stimuli (Fig.II-3D). Therefore, auditory information from A1 is not necessary for the facilitation of reaction time to bimodal stimuli which are integrated in the cortex. On the other hand, activity of V1 was necessary for relative facilitation of reaction to bimodal stimuli (Fig. II-3D) as well as rapid responses to both visual stimuli and bimodal stimuli (Fig. II-3C). Activation of c-Fos in V2L suggests that the audiovisual integration in V2L is proceeded by the convergence of the visual information from V1, at least to some extent, and the auditory information from the regions other than A1 such as the lateral posterior nucleus of the thalamus (Sanderson et al., 1991; Barth et al., 1995), which may potentially have a multisensory property. The convergence of auditory and visual information possibly occurs in the lateral posterior nucleus, as previously observed in another association thalamic nucleus (Komura et al., 2005), and further multisensory processing occurs in the V2L.

4) Role of superior colliculus (SC) for audiovisual behavioral facilitation of reaction time

In addition to that in V2L, enhanced c-Fos expression in the anterior dSC after the audiovisual facilitation was observed. However, SC inactivation deteriorated general responses to all types of

stimuli without affecting the facilitation of reaction time. These results suggest that auditory information and visual information are not integrated in dSC but the audiovisual integration is already conducted in regions upstream of dSC such as V2L and the convergent information in turn drive the activities in dSC to generate facilitated response for head withdrawal from the central hole, resulting in the facilitation of reaction time. To support this idea, c-Fos up-regulation was found in anterior dSC (Fig. I-4) and also in infragranular layers of V2L (Fig. I-3A), which projects to dSC (Thong and Dreher, 1986; Harvey and Worthington, 1990).

This result seems to be inconsistent with previous study which suggests the essential role of the dSC for audiovisual facilitation of spatial orientation accuracy in cats (Burnett et al., 2004). I want to point a few possible explanations for the discrepancy between the previous study and my results. First, the spatial range of inactivation may not have been sufficient to suppress the integrative ability of dSC. I aimed to inactivate only the anterior of one hemispherical SC, where specific up-regulations of c-Fos expression was found after audiovisual facilitation (Fig. II-2B). Even though I cannot completely exclude the possibility of the involvement of the posterior SC in multisensory facilitation, a previous study in cats showed that both rostrally and caudally biased lesions of one hemisphere caused a complete loss of behavioral facilitation (Burnett et al., 2004). Second, the superficial layer of the SC was inactivated accompanied by the inactivation of the dSC in our experiment, which might have affected the audiovisual facilitation (Fig. II-2B). However, my result shows that integration was not blocked by the inactivation of both superficial and deep layers of the SC, suggesting the both layers of SC are not essential for audiovisual facilitation. Third, muscimol may not have been effective in suppressing multisensory neurons in my experiments. However, I observed the increase of reaction time and decrease of the success rate to audiovisual stimuli presented to contralateral hemifield. Thus, multisensory neurons should have been suppressed.

Finally, the neural mechanism that induces multisensory facilitation of reaction time may be different from the mechanism for the spatial orientation accuracy. Because my results suggest that the behavioral indices such as reaction time, movement time, miss error, false hit error are differently

affected by the activities of different brain regions, it is highly likely that the audiovisual facilitation of these different aspects are also differently controlled by different brain regions. My data strongly suggest that the facilitation of reaction time is critically regulated by V2L, whereas SC is critically important for the facilitation of spatial accuracy to audiovisual stimuli as suggested by others (Burnett et al., 2004). In this study, I did not analyze the facilitation of spatial orientation accuracy, because I used relatively high intensity of stimuli, which were easily detected by rats. It is necessary to reveal the differences of neural substrates for the facilitations of different aspects of behavior.

5) Role of lower sensory area in multisensory facilitation

Accumulating evidence suggests multisensory integration in secondary sensory cortical areas in anesthetized rats (Di et al., 1994; Barth et al., 1995; Brett Green et al., 2003; Brett Green et al., 2004; Wallace et al., 2004). However, the behavioral importance of the integration in such early cortical areas was unclarified. Using my newly developed analytical technique for c-Fos mapping, I found that temporally congruent audiovisual stimuli specifically activated the medial region of V2L. Muscimol injection into the region including the medial region of V2L specifically blocked the facilitation of reaction time related to audiovisual integration. I, therefore, suggest that multisensory integration in the early visual area plays an important role on facilitation of reaction time to temporally congruent audiovisual stimuli. This idea is consistent with recent findings that multisensory interactions in the lower-order sensory cortex are characterized by a high degree of temporal precision (Ghazanfar et al., 2005; Lakatos et al., 2007).

One of the major questions concerning multisensory integration is the difference in multisensory processes between the higher- and lower-order sensory cortices (Ghazanfar and Schroeder, 2006). Our results suggest that certain lower-order cortical areas in rats specifically contribute to rapid responses to temporally coincident multisensory stimuli, whereas higher-order cortical areas such as the posterior parietal cortex (area AM in rats (Sanchez et al., 1997; Nakamura, 1999; Tees, 1999)) may

play roles in integrating spatial information on different modality stimuli. Although the role of higher-order cortical areas in our behavioral system remains to be studied, our findings provide evidence for a functional role of a rapid multisensory integration in the lower-order visual cortex.

Figures

Figure II-1.

(A) The auditory (A), visual (V) and congruent audiovisual (cAV) stimuli were randomly presented in a session as cue stimuli (A-V-cAV task) to test the effect of the unilateral injections of saline (SAL) and muscimol (MUS) into the deep layers of the superior colliculus (dSC). (B-D) The average frequencies of errors (false hit and miss, (B)), the average movement time (C) and the average reaction time (D) after unilateral injections of muscimol into one side and that of saline into the other side. Paired *t*-test was performed for the hemisphere ipsilateral and contralateral to the muscimol injection side. (E) Cumulative probabilities for each type of stimulus are presented for the hemifields ipsilateral (left) and contralateral (right) to the muscimol-injection side. The inset in the right figure indicates the audiovisual facilitation index (F_{AV}) for the hemifields ipsilateral and contralateral to the muscimol-injection side. Wilcoxon signed rank test was performed for the responses in the ipsilateral and contralateral hemifields. N.S. = not significant.

Figure II-2.

(A) Representative photomicrographs of the superior colliculus (SC) of rats that performed the auditory, visual and congruent audiovisual (A-V-cAV) task after injecting saline (left) and muscimol (right). # indicates the location of injection tip. Black lines cover the regions where c-Fos expression in grial cells was observed. Black dotted lines indicate the border of deep layers of the superior colliculus (dSC). Scale bars, 1 mm. (B) Coronal diagrams (adapted from Paxinos and Watson, 1997) showing location of injection sites and spread (shown by shaded areas) of muscimol within SC. The injection sites are indicated for the saline-injected (left) and muscimol-injected (right) hemispheres. The extent of c-Fos expression inactivation was identified only in the hemisphere injected with

muscimol. Different densities of shading indicate the degree of suppression of c-Fos expression in regions of individual animals. (C-D) The average densities of c-Fos-positive cells in each ROI (s1-d4, Fig. I-4A) of the anterior (C) and posterior (D) SC of each hemisphere during the performance of the A-V-cAV task after unilateral injections of muscimol and saline into dSC (n=9). Paired t-tests were conducted for saline- and muscimol-injected hemispheres. *P<0.05.

Figure II-3.

(A) The auditory (A), visual (V) and congruent audiovisual (cAV) stimuli were randomly presented in a session as cue stimuli (A-V-cAV task) to test the effect of the bilateral injections of saline (SAL) and muscimol (MUS) into the lateral secondary visual area (V2L), primary visual area (V1) and primary auditory area (A1). (B-C) The success rate (B) and average reaction time (C) in each modality stimulus trial during the performance of the A-V-cAV task after the bilateral injections of saline and muscimol into V2L, V1 and A1. Paired t-test was performed for muscimol and saline injection sessions. *P<0.05. (B) Cumulative probabilities of reaction time for each type of stimulus after bilateral injections of saline and muscimol into V2L, V1, and A1 (yellow areas show audiovisual facilitation index (F_{AV}) see Materials and Methods). The insets in lower figures indicate each F_{AV} and Wilcoxon signed rank test was performed. *P<0.05.

Figure II-4.

(A) Photomicrographs are representative images of c-Fos expression in the lateral secondary visual area (V2L) induced by the performance of the auditory, visual and congruent audiovisual (A-V-cAV) task after saline (SAL) or muscimol (MUS) injection into V2L. Border of muscimol spread estimated by loss of c-Fos expression was shown by dashed line in the muscimol injected section (right side). On some occasions, some gliosis (black arrows) was observed around cannula track (#). Numbers indicate cortical layers, and WM the white matter. Scale bars, 500 μm. (B) Coronal diagrams, adapted from Paxinos and Watson (1997), show the location of the injection sites and the diffusion (shaded areas) of

muscimol for each rat in V2L, primary visual area (V1), and primary auditory area (A1). The regions showing decreased c-Fos expression by muscimol injection are indicated by different densities of shading in individual animals. (C) The bars show the average densities of c-Fos-positive cells in layer 4 of V1, V2L and A1 induced by the performance of the A-V-cAV task after bilateral injections of muscimol (black boxes) or saline (white boxes) into the regions indicated above. Unpaired *t*-tests were performed for saline and muscimol injection conditions in each area. **P*<0.05.

Figure II-5.

(A) Six kinds of cue stimuli (the normal- or low-intensity auditory, visual and congruent audiovisual stimuli) were randomly presented in a session as cue stimuli (N/L A-V-cAV task) to test the effect of the bilateral injections of saline (SAL) and muscimol (MUS) into the lateral secondary visual area (V2L). (B) Reaction times of average unimodal responses under normal- and low-intensity stimulus conditions were compared (Hatched areas show intensity-related unimodal facilitation index (F_{UNI}), see Materials and Methods). The inset in the right figure indicates the F_{UNI} for each experimental animal. (B) Reaction times for audiovisual and faster unimodal responses were compared (Shadowed areas show audiovisual facilitation index (F_{AV})). "Faster (A,V)" indicates maximum unisensory probability at each time point. The insets in the right figure indicate the F_{AV} for each experimental animal. Wilcoxon signed rank test was performed between the saline and muscimol injection sessions. **P*<0.05.

Figure II-6.

(A) Coronal diagrams show the location of the injection sites and the diffusion (shaded areas) of muscimol for each rat in the lateral secondary visual are (V2L). The regions showing decreased c-Fos expression by muscimol injection are indicated by different densities of shading in individual animals. (B) The bars show the average densities of c-Fos-positive cells in layer 4 of V1, V2L and A1 induced

by the performance of the A-V-cAV task after bilateral injections of muscimol (black boxes) or saline (white boxes) into the regions indicated above. Unpaired *t*-tests were performed for saline and muscimol injection conditions in each area. *$P<0.05$.

Fig. II-1

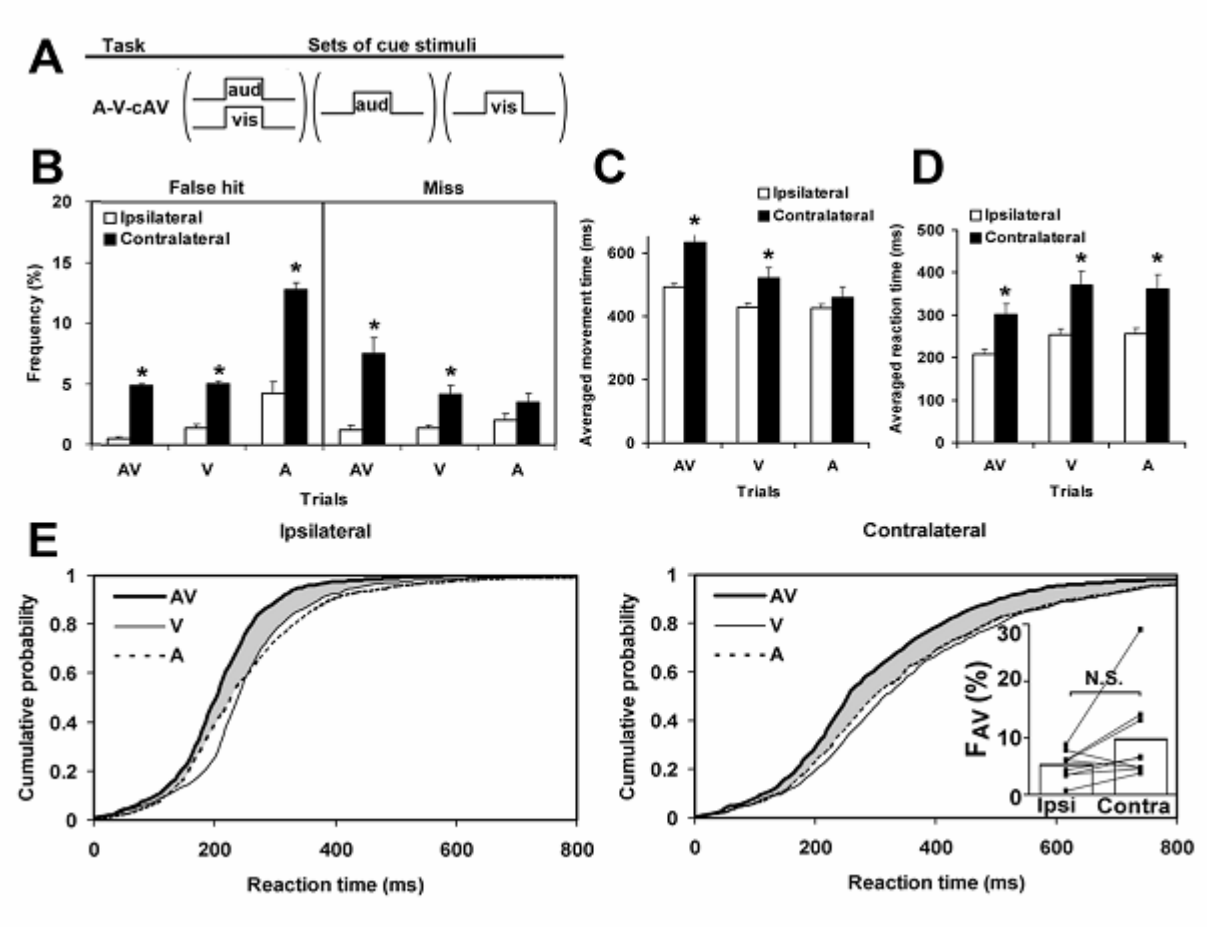
A
Task
Sets of cue stimuli
A-V-cAV
aud
vis
aud
vis
B
False hit
Miss
Ipsilateral
Contralateral
Frequency (%)
AV
V
A
Trials
C
Averaged movement time (ms)
D
Averaged reaction time (ms)
E
Ipsilateral
Contralateral
Cumulative probability
Reaction time (ms)
N.S.
Ipsi
Contra

Fig. II-2

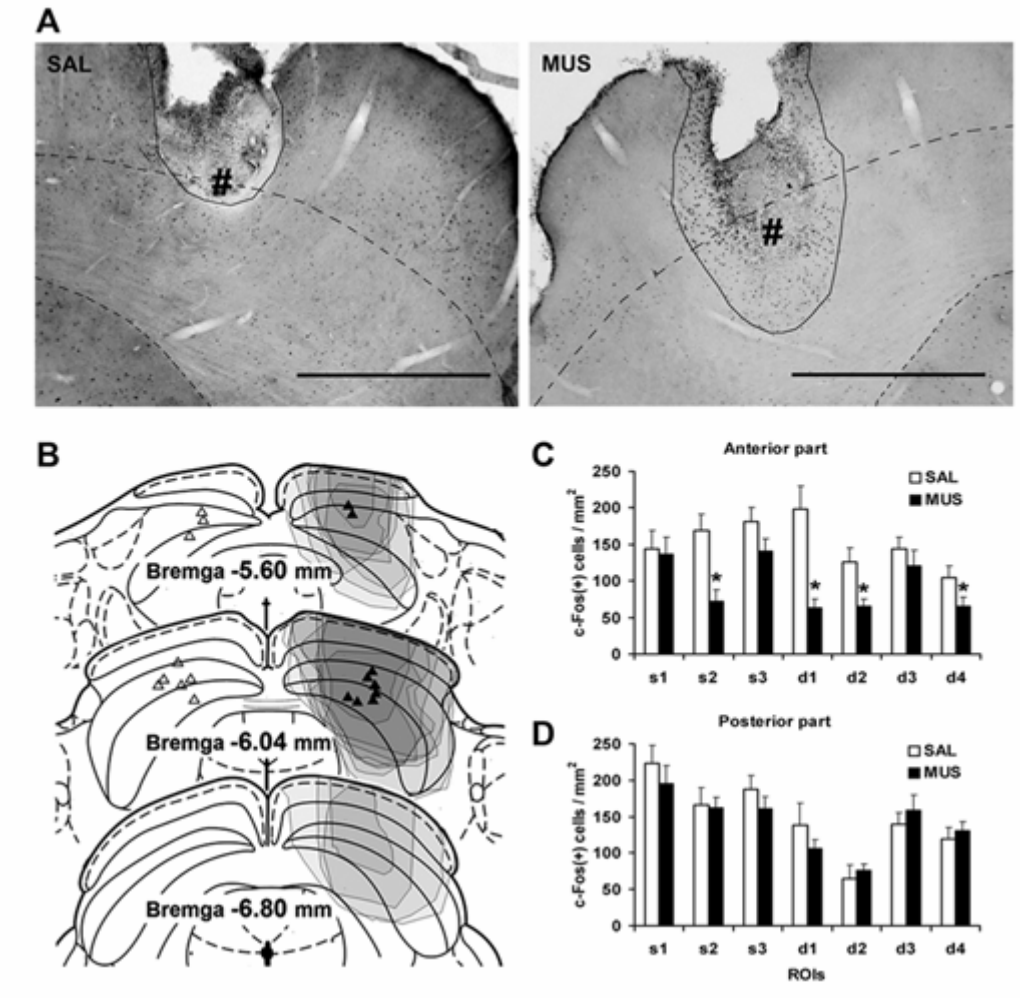
A
SAL
MUS
#
#
B
Bremga -5.60 mm
Bremga -6.04 mm
Bremga -6.80 mm
C
Anterior part
SAL
MUS
c-Fos(+) cells / mm²
250
200
150
100
50
0
s1
s2
s3
d1
d2
d3
d4
D
Posterior part
SAL
MUS
c-Fos(+) cells / mm²
ROIs

Fig. II-3

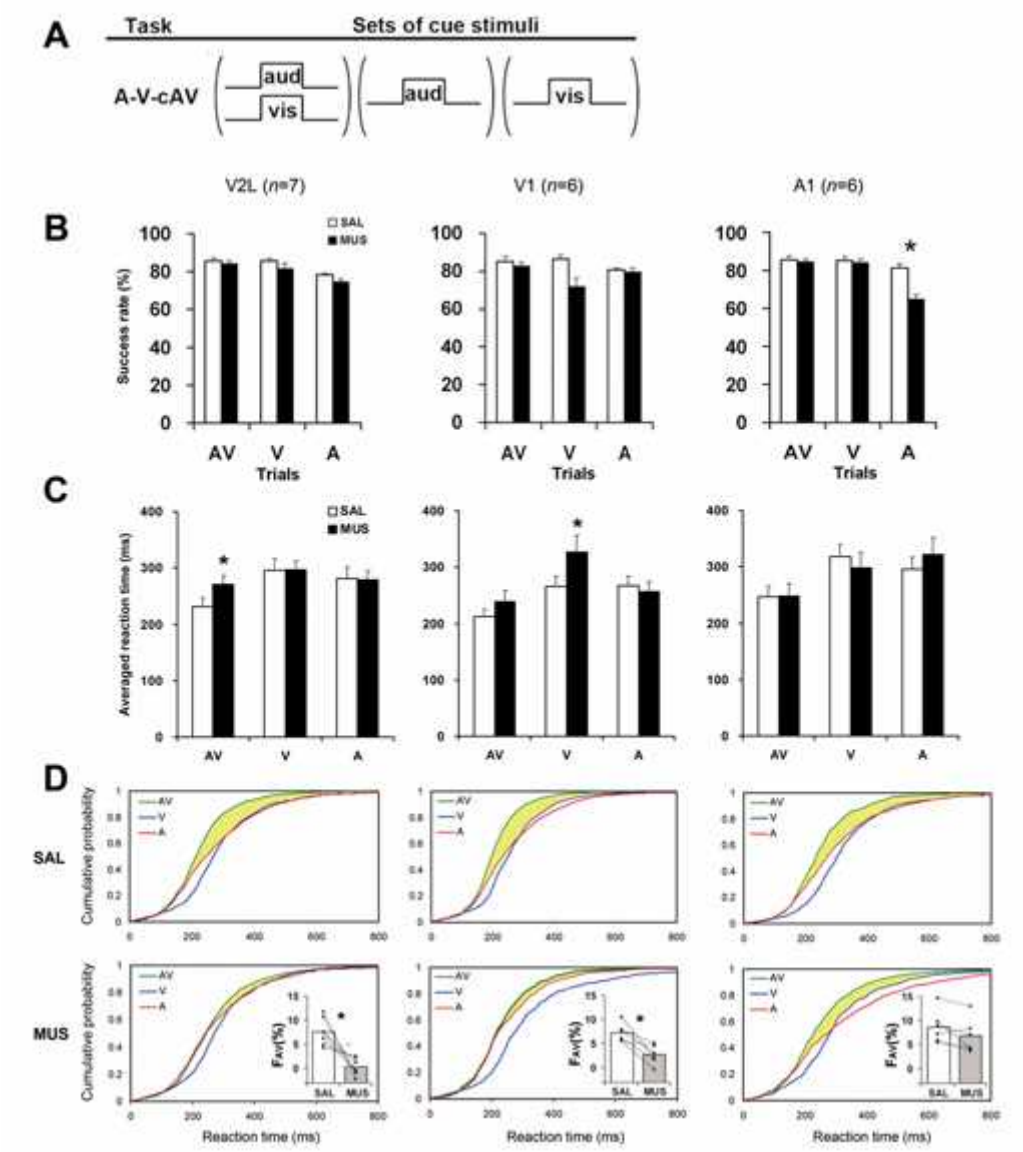
A
Task
Sets of cue stimuli
A-V-cAV
aud
vis
aud
vis
V2L (n=7)
V1 (n=6)
A1 (n=6)
B
SAL
MUS
Success rate (%)
AV
V
A
Trials
C
Averaged reaction time (ms)
D
SAL
MUS
Cumulative probability
Reaction time (ms)
FAV(%)

Fig. II-4

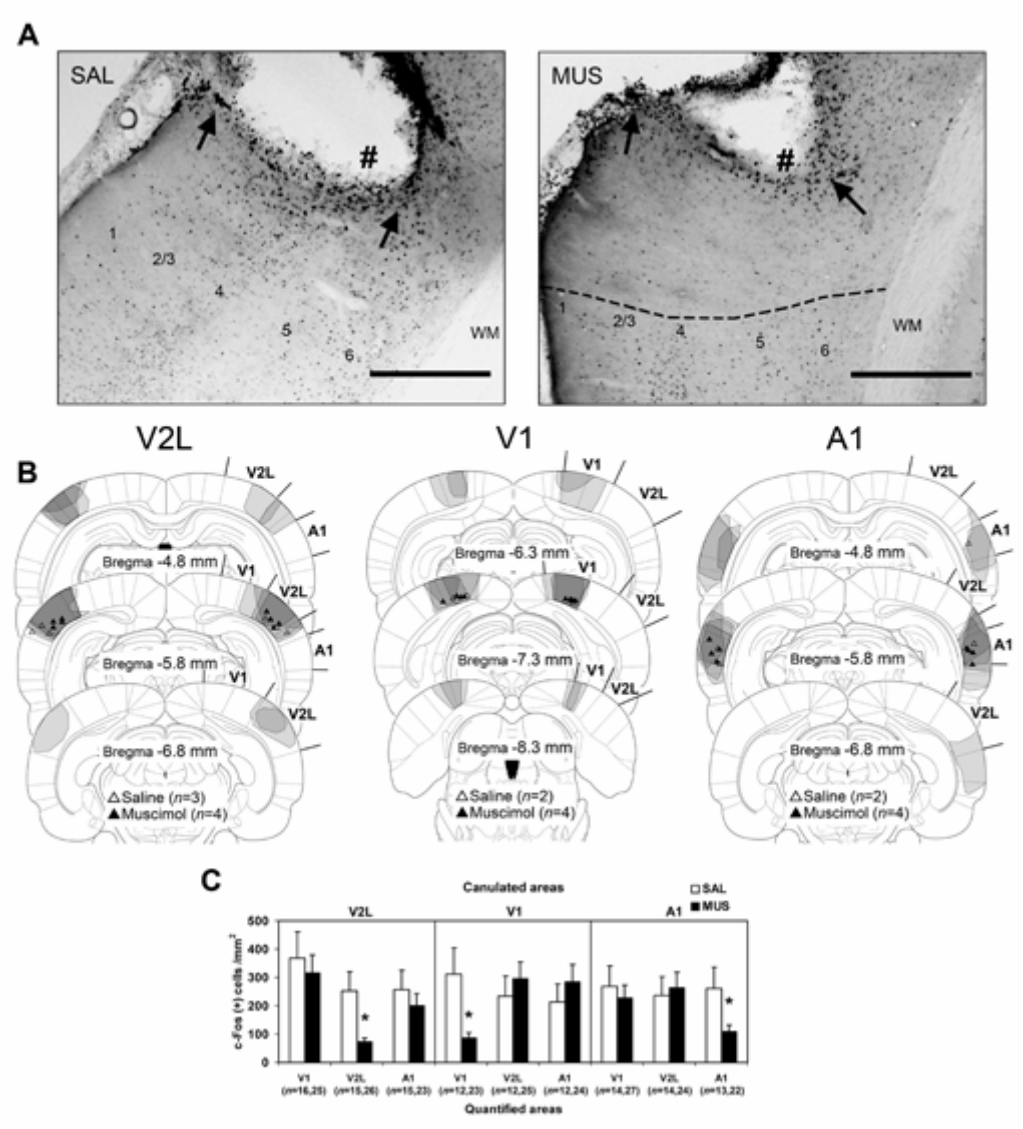
A
SAL
MUS
#
1
2/3
4
5
6
WM
B
V2L
V1
A1
Bregma -4.8 mm
Bregma -5.8 mm
Bregma -6.8 mm
Bregma -6.3 mm
Bregma -7.3 mm
Bregma -8.3 mm
△Saline (n=3)
▲Muscimol (n=4)
△Saline (n=2)
▲Muscimol (n=4)
C
Canulated areas
SAL
MUS
c-Fos (+) cells /mm²
Quantified areas

Fig. II-5

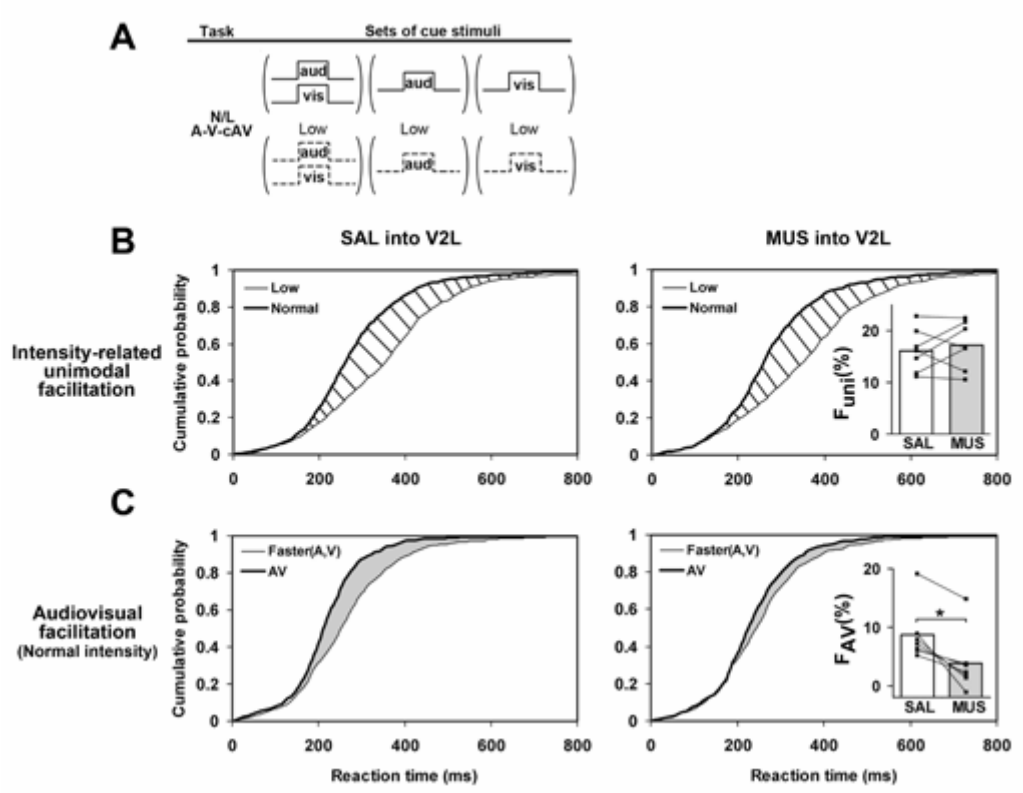
A
Task
Sets of cue stimuli
aud
vis
aud
vis
N/L
A-V-cAV
Low
Low
Low
aud
vis
aud
vis
B
SAL into V2L
MUS into V2L
Intensity-related unimodal facilitation
Cumulative probability
Low
Normal
Low
Normal
Funi(%)
SAL
MUS
C
Audiovisual facilitation
(Normal intensity)
Cumulative probability
Faster(A,V)
AV
Faster(A,V)
AV
FAV(%)
*
SAL
MUS
Reaction time (ms)
Reaction time (ms)

Fig. II-6

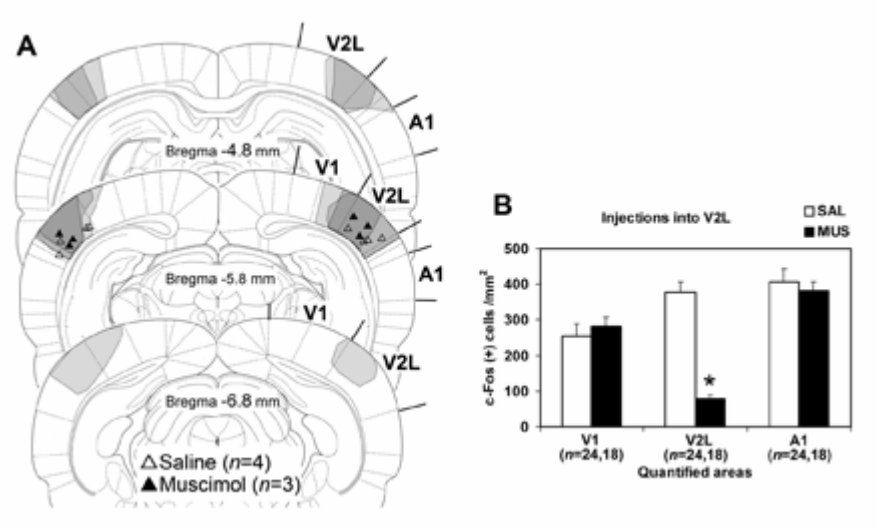
A
V2L
A1
Bregma -4.8 mm
V1
V2L
A1
Bregma -5.8 mm
V1
V2L
Bregma -6.8 mm
△Saline (n=4)
▲Muscimol (n=3)
B
Injections into V2L
SAL
MUS
c-Fos (+) cells /mm²
500
400
300
200
100
0
V1
(n=24,18)
V2L
(n=24,18)
A1
(n=24,18)
Quantified areas

Materials and Methods

Animal treatment and behavioral task

The subjects were 15~16-week-old male Sprague-Dawley rats (*n*=65; SLC, Hamamatsu, Japan), weighing 348-412 g at the onset of the experiment. The animals were housed individually in plastic cages in a 12-h light/dark cycle, and water was provided *ad libitum*. They were fed with sufficient laboratory chow after daily training sessions to maintain more than 90% of their initial weights. They were handled for approximately 2 min/day following behavioral training sessions. All experiments were conducted in accordance with the Guide for the Care and Use of Laboratory Animals (NIH publication number 86-23, 1985) and the guidelines of Okazaki National Research Institutes in Japan.

Behavioral training was conducted in an operant chamber (OP-3501 K; Ohara & Co., Ltd., Tokyo, Japan; 320 × 160 × 450 mm), which was enclosed in a soundproof box (Japan Shield Enclosure, Osaka, Japan) and illuminated by an 8-V direct-current bulb as the house light. The apparatus used in behavioral testing was identical to that used in the previous study (Sakata et al., 2004). Briefly, the apparatus consists of three holes for nose poking with photosensors, a food dispenser in the front wall, and two audiovisual targets on the left and right walls (Fig. I-1A). The audiovisual target is a 6-V direct current bulb placed immediately in front of a loudspeaker so that both visual and auditory stimuli were presented from the same location. The position of each animal's head was controlled such that the animal was able to receive the stimuli at equal distances from the left and right sides when it poked its nose into the central hole. Two intensities of stimuli ("normal" and "low") were used in this study, which were obtained by manipulating applied voltage. Because I focus on the audiovisual facilitation of reaction time rather than two-alternative choice in this study, I used the stimuli that were easily discriminated by rats. The normal-intensity stimuli were set to 11.2 lx for luminescence and 57 dB SPL for sound (broadband noise). The intensities were chosen as high-above-threshold intensity

stimuli with which the rats performed the auditory, visual and congruent audiovisual task (A-V-cAV; in Fig. II-1, II-3) with more than 80% accuracy and also they were able to equally attend to both auditory and visual stimuli, as determined from the similar average reaction times for auditory and visual stimuli. Low-intensity stimuli were set to 0.8 lx for luminescence and 45 dB SPL for sound. These intensities were chosen as above-threshold intensity stimuli with which the rats performed the A-V-cAV task with more than 70% accuracy and also they were able to equally attend to both auditory and visual stimuli (Fig. II-5). All events were controlled using customized software designed by LabVIEW (National Instruments, Austin, TX, USA) on a personal computer.

Training was conducted twice a day as described previously (Sakata et al., 2004). It took 3 to 4 weeks for rats to complete the training. The rats were trained using the two-alternative choice task based on audiovisual cue stimuli slightly modified from that previously described (Sakata et al., 2004, Fig. I-1A). Each trial began with a nose poke into the central hole. After 100 to 400 ms of a random nose poking foreperiod, target stimuli were presented from the left or right side for 1,000 ms. A nose poke into the hole ipsilateral to a cue stimulus within 2,500 ms was immediately rewarded with a food pellet. Errors extinguished the house light for 3,000 ms, designated as the blackout period, and no reward was given. The same trial was repeated after an error (correction procedure). The chance of presenting each stimulus was identical in each session consisting of 300 trials (approximately 50 min). Reaction time was defined as the time from the onset of stimulus presentation to the withdrawal of the nose from the central hole (shaded period in Fig. I-1A).

Behavioral procedure and analyses

c-Fos mapping experiment

The rats were trained in the congruent audiovisual (cAV) task (n=10) or temporally incongruent audiovisual (iAV) task (n=8) (Fig. 1B). In the cAV task, temporally congruent audiovisual stimuli were used as the cue stimuli, whereas in the iAV task, the presentation was randomly delayed for 200 ms

between auditory and visual stimuli. When the rats reached a success rate higher than 75% after more than three training sessions, final test sessions were performed. On testing, all the animals were removed from their home cages with minimal handling and transferred to the task apparatus. About one hour after the beginning of the final test session, rats were immediately perfused for c-Fos immunohistochemistry. The success rate and average reaction time (excluding those in incorrect trials) in the last session were averaged for each group.

Suppression experiments

The rats were trained to perform the A-V-cAV task (Fig. II-1-4) or the normal- or low-intensity auditory, visual, congruent audiovisual (N/L A-V-cAV) task (Fig. II-5). After the animals had mastered each task, they were chronically implanted with cannulae for muscimol application. Each rat performed two to three test sessions under both saline and muscimol injection conditions. After the final test session, rats were sacrificed for c-Fos immunohistochemistry. Behavioral performance was separately analyzed depending on the injection condition, modality and stimulus intensity. The cumulative probability of reaction time was computed for each condition of each rat, and then averaged across rats under the same condition in the same group. The index of audiovisual facilitation of reaction time (F_{AV}) was calculated as the percent increase in response probability during the audiovisual condition compared with that during the faster unimodal condition (i.e. the faster modality response at each time point) in the range of time points from 0 to 800 ms. For calculating intensity-related unimodal facilitation index (F_{UNI}), the cumulative probabilities of normal-intensity unimodal stimuli (the average of auditory and visual stimuli) and low-intensity unimodal stimuli (the average of auditory and visual stimuli) were compared.

c-Fos immunohistochemistry

General description

The rats were deeply anesthetized with sodium pentobarbital (50 mg/kg body weight) and transcardially perfused with 0.9% saline followed by 4% paraformaldehyde. Every fifth coronal section (45 μm thickness) was preserved in two series: one processed for c-Fos immunohistochemistry and the other stained with thionine for the cytoarchitectonic identification of cortical layers and areas. Immunohistochemical analysis was conducted as described previously (Sakata et al., 2002) using rabbit anti-c-Fos antibody (sc-52; Santa Cruz Biotechnology, Santa Cruz, CA, USA) and anti-rabbit IgG (1:1,000 in PBST; Vector Laboratories, Burlingame, CA, USA) with 3,3'-diaminobenzidine (DAB) and nickel as chromogens. Control experiments for nonspecific staining were performed by omitting the primary or secondary antibody (neither of them yielded any positive staining). Control rats (n=6) in their home cages were used to determine the baseline level of c-Fos expression (data not shown).

Digital images (2040 × 1536 pixels) of serial sections (225 μm apart) were captured and digitized in the gray scale with 8 bits using a BX51 (OLYMPUS, Tokyo, Japan) microscope equipped with a DP70 CCD camera interfaced to a PC computer. The images were taken using the 4 × objective. The contrasts of digital images shown were adjusted with Adobe Photoshop after subtracting the background image (blank image) for better visualization.

Quantification of c-Fos-positive cells

Identification of c-Fos signals.

The background of each image was eliminated by subtracting the locally averaged image (the filtering element was 7 × 7 pixels or 15 × 15 μm, which was the largest size of the c-Fos signal). The obtained 8-bit digital images were thresholded to convert them into binary images. The threshold used for each image was set to six times the standard deviation (s.d.) above the average intensity of each cortical section. The images were further processed using a series of morphological filters that enables the identification of a nucleus on the basis of the size of each signal (10-50 pixels) and the ratio (1-3) of

the major and minor axes of an equivalent ellipse, which was fitted to each signal by a least-squares fitting technique using a customized software program designed by LabVIEW. Parameters for the identification of c-Fos-positive nuclei were set such that the automated counts became close to the careful manual counts of several representative sections.

Standardization of images of cortex

The sections that contained artifacts such as tearing or bubbles in the cortex were excluded from the analysis. The entire cortical section was automatically reconstructed from four to eight images (Cecchi et al., 1999). To construct a local density map of c-Fos-positive cells, local c-Fos densities were calculated and mapped using a moving window operator (100 × 100 μm), which scanned pixelwise through an entire image (see Fig. I-2A, B). Image processing was automatically carried out using a customized software program designed by LabVIEW except for identifying the structural landmarks and cutting out image of a large part of the cortex using Adobe Photoshop. Visualizations of standardized maps were carried out using Matlab 7.0 (Mathworks). The standardized cortical section (100 × 1000 pixels, depth × width, respectively) was assigned to one of 16 figures (from Figures 35 to 50; Bregma -4.3 to -8.0 mm) of the standard rat brain atlas (Paxinos and Watson, 1997), as determined from the order of serial sections and the shape of the hippocampus. The averages of 11.5 ±1.58 (mean ±s.d.) sections stained by the anti-c-Fos antibody in each animal were used for this analysis. When there were no available sections that corresponded to one of the 16 figures, those data were generated as the standardized cortical sections by linearly interpolating adjacent serial sections. Post hoc smoothing (spatial averaging) of standardized layer map (1000 × 247 pixels) (width × Bregma distance) was achieved using a moving window operator (20 × 20 pixels). To correct intersubject differences in staining intensity in c-Fos immunohistochemistry, the densities of c-Fos-positive cells in each animal were normalized by linearly adjusting mean - 2 s.d. as 0 % and mean + 2 s.d. as 100 (%). An analysis of the absolute counts (c-Fos-positive cells /mm^2) without normalization also showed

essentially the same results (data not shown). To compare the densities of c-Fos-positive cells across groups of animals, the images of the standardized cortical box or standardized layer-4 map were directly compared on the basis of individual pixels. Statistical comparisons were carried out using the pixelwise running unpaired *t*-test. I chose to set a significance threshold $P < 0.05$ for individual pixels within a minimum of three contiguous sections. The statistical significance for the medial region of V2L was robust for the bin size of a window.

Identification of cytoarchitectonic layers and areas

To determine the location of cortical layers and areas in the standardized sections, I also applied essentially the same procedure to a series of adjacent sections processed by Nissl staining. Digital images (1392 × 1040 pixels) of sections were captured at a low resolution using the 0.75× objective and the background image was subtracted to eliminate the shadowing effect. The resulting images were standardized as described in the above section. The averages of 12.7 ±1.57 (mean ±s.d.) sections stained by the Nissl in each animal were used for this analysis. Staining signals more than - 1 s.d. from the average of each section were used for the analysis. To correct intersubject differences in staining intensity, the staining signals were normalized for each animal by linearly adjusting mean - 1 s.d. as 0 % and mean + 1 s.d. as 100 (%). To reduce the artifact due to staining variance, the normalized pixel values of three adjacent standardized sections were averaged to make one averaged standardized section. Then, the standardized layer 4 map was constructed for each animal and these maps were further averaged for each group of animals or all animals.

ROI (region of interest) analysis for suppression experiments

The areas to be analyzed were determined using Nissl-stained adjacent sections on the basis of the cytoarchitectonic definitions of the primary cortical areas: primary visual area (V1, Bregma 6.3 to 8.3 mm) and primary auditory area (A1, Bregma 4.6 to 6.6 mm) and the region between them: V2L

(Bregma 4.8 to 6.8 mm) (Palomero-Gallagher and Zilles, 2004). Because I found that the decrease in c-Fos expression level after muscimol injection was particularly evident in layer 4, c-Fos-positive cell density (cells /mm^2) in layer 4 was automatically quantified using the identical quantification criteria described above. Minimum of five sections from both hemispheres of each rat were pooled and group-averaged for a given structure for each injection condition. The implantation of cannulae often caused dense c-Fos labeling only around the injector track (see Fig. II-2,4), which may be due to the activation of glial growth (Wang and Redgrave, 1997). When I took ROIs for c-Fos quantification in a section that contained cannula tracks, I avoided those artifacts that were easily discriminated from neurons on the basis of the intensity, location, and morphology of the signal. Some sections were excluded from the quantitative analysis because the artifacts extended into entire target regions.

Surgery and cannulation

The rats (*n*=35) were anesthetized with sodium pentobarbital (50 mg/kg body weights). I targeted V2L, where an increase in c-Fos expression level was observed after the cAV task, for the inactivation with muscimol. Stainless steel guide cannulae (27 gauge, 0.45 mm o.d.) were bilaterally implanted into one of the three brain regions using the following coordinates: (i) V2L (*n*=7 for Exp. 2 and *n*=7 for Exp. 3, respectively), 5.8 mm caudal to Bregma, 6.0 mm lateral to the midline, and 0.6 mm ventral from the dural surface; (ii) A1 (*n*=6), 5.6 mm caudal to Bregma, 6.7 mm lateral to the midline, and 1.4 mm ventral from the dural surface; (iii) V1 (*n*=6), 7.3 mm caudal to Bregma, 3.3-3.7 mm lateral to the midline, and 0.6 mm ventral from the dural surface; (iv) anterior dSC (intermediate/deep layer of superior colliculus, *n*=9), 5.8 mm caudal to Bregma, 1.4 mm lateral to the midline, and 3.2 mm ventral to the dural surface. Note that I set the target region of V1 away fromV2L carefully to avoid the suppression of V2L when V1 was injected with muscimol. The cannulae were fixed with dental cement, and wire stylets were inserted into the guide cannulae to prevent their blockage. The rats were allowed one week to recover before starting the experiments. Only animals with cannula tips correctly

located within targeted structures were included in the study.

Muscimol microinfusion

I analyzed the effect of reversible inactivation of brain sites on the performance of behavioral tasks using muscimol, which transiently suppresses the activity of excitatory neurons by activating GABA A receptors on the surface of neurons without affecting passing fibers (Martin and Ghez, 1999; Majchrzak and Di Scala, 2000). One week after the surgery, the rats were tested again to ensure that they could perform the task properly. On the test day, the rats were restrained by hand and received bilateral microinfusions of either saline or muscimol (1000 ng in 0.5 μl of 0.9% saline for cortices, 25 ng in 0.5 μl of 0.9% saline for dSC) through an inner cannula (35 gauge, 0.2 mm o.d.). For dSC injection, the rats received simultaneous injections of muscimol into one of dSCs and the saline into the contralateral side of dSC. Injection of high doses of muscimol (>50 ng) produced a severe circling behavior toward the side ipsilateral to the site of muscimol injection and did not allow the rats to start the task. The dose of 25 ng was necessary and sufficient to observe the contralateral neglect effect, which is a behavioral consequence of a unilateral SC lesion (Stein and Meredith, 1993). I did not observe any behavioral abnormalities in the rats after the injections of muscimol at this amount. Similar concentrations were used in other studies to examine the behavioral effect of muscimol injected into the cortex (Kim and Ragozzino, 2005) and SC (Kilpatrick et al., 1982; Wang and Redgrave, 1997). The tip of the inner cannula extended 0.6 mm below the guide cannula. A 10-μl Hamilton syringe connected to an infusion pump was used to deliver 0.5 μl of muscimol (Sigma) or saline over a period of 2 min. The inner cannulae were left in place for another 2 min to allow the diffusion of the solution. After the infusion and a 30-min rest period in home cages, the rats performed the A-V-cAV task. Each rat was tested only once per day. Two or three injection sessions were conducted for each injection condition in each rat. Training sessions were introduced between injection sessions to ensure that the rats performed the task properly.

Injections of muscimol or saline vehicle into each brain region were made through an inner cannula (35 gauge, 0.2 mm o.d.). The tip of the inner cannula extended 0.6 mm below the guide cannula. A 10-μl Hamilton syringe connected to an infusion pump was used to deliver 0.5 μl of muscimol (Sigma) or 0.9% saline over a period of 2 min. The inner cannulae were left in place for another 2 min to allow the diffusion of the solution. After the infusion and a 30-min rest period in home cages, the rats performed the A-V-cAV task. Each rat was tested only once per day. Two or three injection sessions were conducted for each injection condition in each rat. The side that received the unilateral muscimol injection was alternatively changed for SC. Training sessions were introduced between injection sessions to ensure that the rats performed the task properly. The rats were sacrificed after the final injection sessions for immunohistochemistry (cortices; 3 to 4 rats for muscimol and 2 to 3 rats for saline in each injection group, SC: simultaneous unilateral injections (n=9) of muscimol and saline).

Statistical analysis

All data are presented as mean plus and minus standard errors (s.e.), unless otherwise stated. All the statistical analyses of collected data except for analysis of the standardization method were conducted using STATISTICA (StatSoft Japan Inc., Tokyo, Japan). For behavioral data, one-way repeated measures analysis o f variance (ANOVA) was used to analyze individual conditions, and the Tukey HSD test for post hoc comparison was used for pair-wise comparisons among modality conditions. For F_{AV} and F_{UNI} data, nonparametric (Wilcoxon signed rank) tests were used because the data were not normally distributed. Otherwise, the unpaired *t*-test or paired *t*-test was used (two-tailed). A probability value of < 0.05 was considered significant.

Acknowledgements

This thesis was supported by many people.

I greatly thank Prof. Yamamori in the National Institute for Basic Biology (NIBB) for providing the chance and environment to investigate exciting research. I thank Dr. Sakata in the Rutgers University for his general and technical advices. I thank Dr. Bosch in brain institute at MIT for his helpful advices and technical contribution for muscimol experiment. I thank Prof. Sakurai in Kyoto University for encouragement and technical suggestions. I thank Toru Nakamura for valuable help with initiating the muscimol experiment and Drs. Yasunori Hayashi and Akiya Watakabe for helpful comments on early drafts of the manuscript. I thank other members of the Division of Brain Biology in NIBB for their wisdom and technical supports and advices. And I greatly appreciate my parents, grandparents and brothers for their financial and mental supports all through my life.

Finally, I am grateful and pray for the sacrifice of many experimental animals.

References

Angelucci A, Bullier J (2003) Reaching beyond the classical receptive field of V1 neurons: horizontal or feedback axons? J Physiol Paris 97:141-154.

Barth DS, Goldberg N, Brett B, Di S (1995) The spatiotemporal organization of auditory, visual, and auditory-visual evoked potentials in rat cortex. Brain Res 678:177-190.

Bell AH, Meredith MA, Van Opstal AJ, Munoz DP (2005) Crossmodal integration in the primate superior colliculus underlying the preparation and initiation of saccadic eye movements. J Neurophysiol 93:3659-3673.

Berninger B, Guillemot F, Gotz M (2007) Directing neurotransmitter identity of neurones derived from expanded adult neural stem cells. Eur J Neurosci 25:2581-2590.

Bolognini N, Frassinetti F, Serino A, Ladavas E (2005) "Acoustical vision" of below threshold stimuli: interaction among spatially converging audiovisual inputs. Exp Brain Res 160:273-282.

Brett Green B, Fifkova E, Larue DT, Winer JA, Barth DS (2003) A multisensory zone in rat parietotemporal cortex: intra- and extracellular physiology and thalamocortical connections. J Comp Neurol 460:223-237.

Brett Green B, Paulsen M, Staba RJ, Fifkova E, Barth DS (2004) Two distinct regions of secondary somatosensory cortex in the rat: topographical organization and multisensory responses. J Neurophysiol 91:1327-1336.

Bronchti G, Heil P, Sadka R, Hess A, Scheich H, Wollberg Z (2002) Auditory activation of "visual" cortical areas in the blind mole rat (Spalax ehrenbergi). Eur J Neurosci 16:311-329.

Brosch M, Selezneva E, Scheich H (2005) Nonauditory events of a behavioral procedure activate auditory cortex of highly trained monkeys. J Neurosci 25:6797-6806.

Burnett LR, Stein BE, Chaponis D, Wallace MT (2004) Superior colliculus lesions preferentially disrupt multisensory orientation. Neuroscience 124:535-547.

Bushnell PJ, Benignus VA, Case MW (2003) Signal detection behavior in humans and rats: a comparison with matched tasks. Behav Processes 64:121-129.

Calvert GA, Bullmore ET, Brammer MJ, Campbell R, Williams SC, McGuire PK, Woodruff PW, Iversen SD, David AS (1997) Activation of auditory cortex during silent lipreading. Science 276:593-596.

Campi KL, Karlen SJ, Bales KL, Krubitzer L (2007) Organization of sensory neocortex in prairie voles (Microtus ochrogaster). J Comp Neurol 502:414-426.

Cecchi GA, Ribeiro S, Mello CV, Magnasco MO (1999) An automated system for the mapping and quantitative analysis of immunocytochemistry of an inducible nuclear protein. J Neurosci Methods 87:147-158.

Coogan TA, Burkhalter A (1993) Hierarchical organization of areas in rat visual cortex. J Neurosci 13:3749-3772.

Corneil BD, Van Wanrooij M, Munoz DP, Van Opstal AJ (2002) Auditory-visual interactions

subserving goal-directed saccades in a complex scene. J Neurophysiol 88:438-454.

Dean P, Redgrave P (1984) The superior colliculus and visual neglect in rat and hamster. II. Possible mechanisms. Brain Res 320:143-153.

Dean P, Mitchell IJ, Redgrave P (1988) Responses resembling defensive behaviour produced by microinjection of glutamate into superior colliculus of rats. Neuroscience 24:501-510.

Dean P, Mitchell IJ, Redgrave P (1988) Contralateral head movements produced by microinjection of glutamate into superior colliculus of rats: evidence for mediation by multiple output pathways. Neuroscience 24:491-500.

Di S, Brett B, Barth DS (1994) Polysensory evoked potentials in rat parietotemporal cortex: combined auditory and somatosensory responses. Brain Res 642:267-280.

Espinoza SG, Thomas HC (1983) Retinotopic organization of striate and extrastriate visual cortex in the hooded rat. Brain Res 272:137-144.

Farivar R, Zangenehpour S, Chaudhuri A (2004) Cellular-resolution activity mapping of the brain using immediate-early gene expression. Front Biosci 9:104-109.

Felleman DJ, Van Essen DC (1991) Distributed hierarchical processing in the primate cerebral cortex. Cereb Cortex 1:1-47.

Frens MA, Van Opstal AJ (1995) A quantitative study of auditory-evoked saccadic eye movements in two dimensions. Exp Brain Res 107:103-117.

Gerstein GL, Kirkland KL, Musial PG, Talwar SK (2002) Recordings, behaviour and models related to corticothalamic feedback. Philos Trans R Soc Lond B Biol Sci 357:1835-1841.

Ghazanfar AA, Maier JX, Hoffman KL, Logothetis NK (2005) Multisensory integration of dynamic faces and voices in rhesus monkey auditory cortex. J Neurosci 25:5004-5012.

Ghazanfar AA, Schroeder CE (2006) Is neocortex essentially multisensory? Trends Cogn Sci. 10:278-285.

Giard MH, Peronnet F (1999) Auditory-visual integration during multimodal object recognition in humans: a behavioral and electrophysiological study. J Cogn Neurosci 11:473-490.

Goodale MA, Murison RC (1975) The effects of lesions of the superior colliculus on locomotor orientation and the orienting reflex in the rat. Brain Res 88:243-261.

Hairston WD, Hodges DA, Burdette JH, Wallace MT (2006) Auditory enhancement of visual temporal order judgment. Neuroreport 17:791-795.

Harvey AR, Worthington DR (1990) The projection from different visual cortical areas to the rat superior colliculus. J Comp Neurol 298:281-292.

Holmes NP, Spence C (2005) Multisensory integration: space, time and superadditivity. Curr Biol 15:R762-764.

Hughes HC, Reuter Lorenz PA, Nozawa G, Fendrich R (1994) Visual-auditory interactions in sensorimotor processing: saccades versus manual responses. J Exp Psychol Hum Percept Perform 20:131-153.

Jiang W, Jiang H, Stein BE (2002) Two corticotectal areas facilitate multisensory orientation behavior. J Cogn Neurosci 14:1240-1255.

Johnson RR, Burkhalter A (1996) Microcircuitry of forward and feedback connections within rat visual cortex. J Comp Neurol 368:383-398.

Johnson RR, Burkhalter A (1997) A polysynaptic feedback circuit in rat visual cortex. J Neurosci 17:7129-7140.

Kayser C, Petkov CI, Augath M, Logothetis NK (2005) Integration of touch and sound in auditory cortex. Neuron 48:373-384.

Kayser C, Petkov CI, Augath M, Logothetis NK (2007) Functional imaging reveals visual modulation of specific fields in auditory cortex. J Neurosci 27:1824-1835.

Kilpatrick IC, Collingridge GL, Starr MS (1982) Evidence for the participation of nigrotectal gamma-aminobutyrate-containing neurones in striatal and nigral-derived circling in the rat. Neuroscience 7:207-222.

Kim J, Ragozzino ME (2005) The involvement of the orbitofrontal cortex in learning under changing task contingencies. Neurobiol Learn Mem 83:125-133.

King AJ, Palmer AR (1985) Integration of visual and auditory information in bimodal neurones in the guinea-pig superior colliculus. Exp Brain Res 60:492-500.

Koch M, Schnitzler HU (1997) The acoustic startle response in rats--circuits mediating evocation, inhibition and potentiation. Behav Brain Res 89:35-49.

Komura Y, Tamura R, Uwano T, Nishijo H, Ono T (2005) Auditory thalamus integrates visual inputs into behavioral gains. Nat Neurosci 8:1203-1209.

Lakatos P, Chen CM, O'connell MN, Mills A, Schroeder CE (2007) Neuronal oscillations and multisensory interaction in primary auditory cortex. Neuron 53:279-292.

Lein ES, Hawrylycz MJ, Ao N, Ayres M, Bensinger A, Bernard A, Boe AF, Boguski MS, Brockway KS, Byrnes EJ, Chen L, Chen L, Chen TM, Chi Chin M, Chong J, Crook BE, Czaplinska A, Dang CN, Datta S, Dee NR et al. (2006) Genome-wide atlas of gene expression in the adult mouse brain. Nature 445:168-176.

Leitner DS, Cohen ME (1985) Role of the inferior colliculus in the inhibition of acoustic startle in the rat. Physiol Behav 34:65-70.

Macaluso E, Frith CD, Driver J (2000) Modulation of human visual cortex by crossmodal spatial attention. Science 289:1206-1208.

Majchrzak M, Di Scala G (2000) GABA and muscimol as reversible inactivation tools in learning and memory. Neural Plast 7:19-29.

Martin JH, Ghez C (1999) Pharmacological inactivation in the analysis of the central control of movement. J Neurosci Methods 86:145-159.

McDaniel WF, Coleman J, Lindsay JF Jr (1982) A comparison of lateral peristriate and striate neocortical ablations in the rat. Behav Brain Res 6:249-272.

Meredith MA, Stein BE (1985) Descending efferents from the superior colliculus relay integrated multisensory information. Science 227:657-659.

Meredith MA, Stein BE (1986) Visual, auditory, and somatosensory convergence on cells in superior colliculus results in multisensory integration. J Neurophysiol 56:640-662.

Meredith MA, Nemitz JW, Stein BE (1987) Determinants of multisensory integration in superior colliculus neurons. I. Temporal factors. J Neurosci 7:3215-3229.

Meredith MA, Stein BE (1996) Spatial determinants of multisensory integration in cat superior colliculus neurons. J Neurophysiol 75:1843-1857.

Mermelstein PG, Bito H, Deisseroth K, Tsien RW (2000) Critical dependence of cAMP response element-binding protein phosphorylation on L-type calcium channels supports a selective response to EPSPs in preference to action potentials. J Neurosci 20:266-273.

Miller J (1982) Divided attention: evidence for coactivation with redundant signals. Cognit Psychol 14:247-279.

Molholm S, Ritter W, Murray MM, Javitt DC, Schroeder CE, Foxe JJ (2002) Multisensory auditory-visual interactions during early sensory processing in humans: a high-density electrical mapping study. Brain Res Cogn Brain Res 14:115-128.

Montero VM (1993) Retinotopy of cortical connections between the striate cortex and extrastriate visual areas in the rat. Exp Brain Res 94:1-15.

Murray MM, Foxe JJ, Higgins BA, Javitt DC, Schroeder CE (2001) Visuo-spatial neural response interactions in early cortical processing during a simple reaction time task: a high-density electrical mapping study. Neuropsychologia. 39:828-844.

Murray MM, Molholm S, Michel CM, Heslenfeld DJ, Ritter W, Javitt DC, Schroeder CE, Foxe JJ (2005) Grabbing your ear: rapid auditory-somatosensory multisensory interactions in low-level sensory cortices are not constrained by stimulus alignment. Cereb Cortex 15:963-974.

Nakamura K (1999) Auditory spatial discriminatory and mnemonic neurons in rat posterior parietal cortex. J Neurophysiol 82:2503-2517.

Nguyen PT, Holschneider DP, Maarek JM, Yang J, Mandelkern MA (2004) Statistical parametric mapping applied to an autoradiographic study of cerebral activation during treadmill walking in rats. Neuroimage 23:252-259.

Olavarria J, Van Sluyters RC (1982) The projection from striate and extrastriate cortical areas to the superior colliculus in the rat. Brain Res. 242:332-336.

Olavarria J, Montero VM (1984) Relation of callosal and striate-extrastriate cortical connections in the rat: morphological definition of extrastriate visual areas. Exp Brain Res 54:240-252.

Palomero-Gallagher, N., Zilles, K. (2004) The rat isocortex. In: Paxinos, G.: The Rat Nervous System. Academic Press, San Diego pp :729-757.

Patching GR, Quinlan PT (2004) Cross-modal integration of simple auditory and visual events. Percept Psychophys 66:131-140.

Paxinos G, Watson C (1997) The Rat Brain in Stereotaxic Coordinates (3rd ed.). Academic Press, :Sydney.

Peck CK (1996) Visual-auditory integration in cat superior colliculus: implications for neuronal control of the orienting response. Prog Brain Res 112:167-177.

Piche M, Robert S, Miceli D, Bronchti G (2004) Environmental enrichment enhances auditory takeover of the occipital cortex in anophthalmic mice. Eur J Neurosci 20:3463-3472.

Pinto Hamuy T, Montero VM, Torrealba F (2004) Neurotoxic lesion of anteromedial/posterior parietal cortex disrupts spatial maze memory in blind rats. Behav Brain Res 153:465-470.

Populin LC, Yin TC (2002) Bimodal interactions in the superior colliculus of the behaving cat. J Neurosci 22:2826-2834.

Populin LC (2005) Anesthetics change the excitation/inhibition balance that governs sensory processing in the cat superior colliculus. J Neurosci 25:5903-5914.

Redgrave P, Dean P, Souki W, Lewis G (1981) Gnawing and changes in reactivity produced by microinjections of picrotoxin into the superior colliculus of rats. Psychopharmacology (Berl) 75:198-203.

Rutkowski RG, Weinberger NM (2005) Encoding of learned importance of sound by magnitude of representational area in primary auditory cortex. Proc Natl Acad Sci USA. 102:13664-13669.

Sahibzada N, Dean P, Redgrave P (1986) Movements resembling orientation or avoidance elicited by electrical stimulation of the superior colliculus in rats. J Neurosci 6:723-733.

Sakata S, Kitsukawa T, Kaneko T, Yamamori T, Sakurai Y (2002) Task-dependent and cell-type-specific Fos enhancement in rat sensory cortices during audio-visual discrimination. Eur J Neurosci 15:735-743.

Sakata S, Yamamori T, Sakurai Y (2004) Behavioral studies of auditory-visual spatial recognition and integration in rats. Exp Brain Res 159:409-417.

Sakowitz OW, Quian Quiroga R, Schurmann M, Basar E (2005) Spatio-temporal frequency characteristics of intersensory components in audiovisually evoked potentials. Brain Res Cogn Brain Res 23:316-326.

Sanchez RF, Montero VM, Espinoza SG, Diaz E, Canitrot M, Pinto Hamuy T (1997) Visuospatial discrimination deficit in rats after ibotenate lesions in anteromedial visual cortex. Physiol Behav 62:989-994.

Sanderson KJ, Dreher B, Gayer N (1991) Prosencephalic connections of striate and extrastriate areas of rat visual cortex. Exp Brain Res 85:324-334.

Schleicher A, Zilles K (1990) A quantitative approach to cytoarchitectonics: analysis of structural inhomogeneities in nervous tissue using an image analyser. J Microsc 157:367-381.

Schroeder CE, Foxe JJ (2002) The timing and laminar profile of converging inputs to multisensory areas of the macaque neocortex. Brain Res Cogn Brain Res 14:187-198.

Schroger E, Widmann A (1998) Speeded responses to audiovisual signal changes result from bimodal integration. Psychophysiology 35:755-759.

Smith AL, Parsons CH, Lanyon RG, Bizley JK, Akerman CJ, Baker GE, Dempster AC, Thompson ID, King AJ (2004) An investigation of the role of auditory cortex in sound localization using muscimol-releasing Elvax. Eur J Neurosci 19:3059-3072.

Stein BE, Huneycutt WS, Meredith MA (1988) Neurons and behavior: the same rules of multisensory integration apply. Brain Res 448:355-358.

Stein BE., Meredith MA., Huneycutt WS. & McDade L. (1989) Behavioral indices of multisensory integration: orientation to visual cues is affected by auditory stimuli. J. Cogn. Neurosci., 1:12-24.

Stein BE, Meredith MA (1993) The merging of the senses. MIT Press, :Cambridge.

Stein BE (1998) Neural mechanisms for synthesizing sensory information and producing adaptive behaviors. Exp Brain Res 123:124-135.

Talwar SK, Musial PG, Gerstein GL (2001) Role of mammalian auditory cortex in the perception of elementary sound properties. J Neurophysiol 85:2350-2358.

Tees RC (1999) The effects of posterior parietal and posterior temporal cortical lesions on multimodal spatial and nonspatial competencies in rats. Behav Brain Res 106:55-73.

Thong IG, Dreher B (1986) The development of the corticotectal pathway in the albino rat. Brain Res. 390:227-238.

Toldi J, Feher O, Wolff JR (1986) Sensory interactive zones in the rat cerebral cortex. Neuroscience. 18:461-465.

van Atteveldt N, Formisano E, Goebel R, Blomert L (2004) Integration of letters and speech sounds in the human brain. Neuron 43:271-282.

Wada M, Yoshimi K, Higo N, Ren YR, Mochizuki H, Mizuno Y, Kitazawa S (2006) Statistical parametric mapping of immunopositive cell density. Neurosci Res. 56:96-102.

Wallace MT, Ramachandran R, Stein BE (2004) A revised view of sensory cortical parcellation. Proc Natl Acad Sci USA 101:2167-2172.

Wang S, Redgrave P (1997) Microinjections of muscimol into lateral superior colliculus disrupt orienting and oral movements in the formalin model of pain. Neuroscience 81:967-988.

Wenger MJ, Townsend JT (2000) Basic response time tools for studying general processing capacity in attention, perception, and cognition. J Gen Psychol. 127:67-99.

Whitchurch EA, Takahashi TT (2006) Combined Auditory and Visual Stimuli Facilitate Head Saccades in the Barn Owl (Tyto alba). J Neurophysiol. 96:730-745.

Wilent WB, Contreras D (2004) Synaptic responses to whisker deflections in rat barrel cortex as a function of cortical layer and stimulus intensity. J Neurosci 24:3985-3998.

Wilkinson LK, Meredith MA, Stein BE (1996) The role of anterior ectosylvian cortex in cross-modality orientation and approach behavior. Exp Brain Res 112:1-10.

Zangenehpour S, Chaudhuri A (2001) Neural activity profiles of the neocortex and superior colliculus after bimodal sensory stimulation. Cereb Cortex 11:924-935.

Zilles K, Zilles B, Schleicher A (1980) A quantitative approach to cytoarchitectonics. VI. The areal pattern of the cortex of the albino rat. Anat Embryol (Berl) 159:335-360.

Zilles K, Wree A, Schleicher A, Divac I (1984) The monocular and binocular subfields of the rat's primary visual cortex: a quantitative morphological approach. J Comp Neurol 226:391-402.

Abbreviations

A1, primary auditory area; ANOVA, analysis of variance; A-V-cAV; auditory, visual and congruent audiovisual stimuli; AuD, secondary auditory cortex, dorsal area; cAV, congruent audiovisual stimuli; DAB, 3,3'-diaminobenzidine; dSC, deep layers of superior colliculus; GLI, gray level index; iAV, temporally incongruent audiovisual stimuli; IC, inner contour; LV, lateroventral end; MD, mediodorsal end; OC, outer contour; PBS, phosphate buffered saline; PBST, 0.1M PBS containing 0.2% Triton X-100; PFA, 4% paraformaldehyde in 0.1 M PBS; ROI, region of interest; PtA, parietal association cortex; s.e., standard error; s.d., standard deviation; SC, superior colliculus; TeA, temporal association cortex; V1, primary visual area; V2L, lateral secondary visual area